A methodological platform to study molecular biocompatibility of biomaterials

Experimental and clinical studies

Maria Lennerås

Department of Biomaterials
Institute of Clinical Sciences
Sahlgrenska Academy at University of Gothenburg

UNIVERSITY OF GOTHENBURG

Gothenburg 2016

Cover illustration: Cellular extension of a human mesenchymal stem cell interacting with surface features of an oxidised titanium implant

A methodological platform to study molecular biocompatibility of biomaterials

maria.lenneras@gu.se

ISBN 978-91-628-9817-5

Printed in Gothenburg, Sweden 2016
Ineko AB

Ex labore fructus

ABSTRACT

The aim of this project was to develop a methodological platform in order to advance our scientific understanding of the mechanisms of osseointegration. Screw-shaped, titanium implants, with different surface properties, were inserted in the rat tibia, or incubated in mono- or co-culture of human monocytes and MSCs. After different time points, the implant-adherent cells or the peri-implant bone were harvested and processed for different analyses. For *in-vivo* studies, qPCR, immunohistochemistry, histomorphometry, electron microscopy and removal torque analyses were used. In the *in-vitro* study, FACS, qPCR, ELISA and protein profiling were applied. Finally, qPCR was employed in a clinical study to analyse the abutment-adherent cells of osseointegrated fixtures. At the early time points *in vivo*, a higher gene expression of MSC recruitment and adhesion factors (CXCR4 and integrin-β1) was found in cells adhering to the oxidised compared to machined implant. This was corroborated by predominance of MSCs at the oxidised surface, as judged by immunohistochemistry and SEM. At the later time points, cells adhering to oxidised implants retained a higher expression of bone formation (ALP and OC) and bone remodelling (TRAP and CatK) genes. The qPCR findings correlated with histomorphometric, electron microscopy and removal torque measurements, revealing progressively increasing bone-implant contact and bone bonding and, as a result, an increase in the biomechanical stability of the oxidised implant. The enhanced RANKL/OPG expression ratio corresponded to the remodelling phase at the bone-implant interface. The qPCR analysis of FACS-sorted cells showed that the co-existence of monocytes and MSCs on the implant surface, *in vitro*, upregulates the gene expression of some cytokines in a cell-specific manner. The clinical study showed that bacterial colonisation was frequently detected on the skin, the abutment and in the bone canal. A higher expression of TNF-α was associated with positive cultures of *S. aureus*, whereas fixture loss was associated with lower expression of OC and IL-10.

In conclusion, the present methodological platform enables detailed analyses of the events at the bone-implant interface. Employing this platform demonstrated that implant surface properties elicit a cellular and molecular cascade for rapid cell recruitment and enhanced bone formation and remodelling, which accelerates bone maturation and implant stability. Finally, the results of the thesis provide a first line of information on factors that could affect the performance of percutaneous implants.

Keywords: Osseointegration, titanium, inflammation, cell recruitment, cell adhesion, bone regeneration, bone remodelling, gene expression, immunohistochemistry, histomorphometry, removal torque, ultrastructure, FACS, protein profiling, transfemoral amputation, abutment, percutaneous, bacteria, clinical signs.

ISBN: 978-91-628-9817-5

SAMMANFATTNING PÅ SVENSKA

Att förlorade tänder kan ersättas med titanimplantat är vida känt, men vilka biologiska faktorer som ligger bakom benbildningen vid implantatytan är ännu inte klarlagt. Syftet med avhandlingen var att utveckla en metodplattform för att i detalj kunna studera de cellulära och molekylära processerna som styr inflammation, benbildning och benremodellering vid implantatytan.Titanimplantat med olika ytegenskaper sattes i skenbenet på råtta och cellerna på skruvarna, samt det omkringliggande benet, analyserades vid olika tidpunkter med qPCR, immunohistokemi, histologi, histomorfometri elektronmikroskopi och urvridningstest. Specifika cellulära processer undersöktes i provrörsmiljö och analyserades med FACS, qPCR, ELISA och proteinprofilering. Genuttryck i celler som var adherenta till hudpenetrerande distanser hos lårbensamputerade patienter med benförankrade implantat analyserades med qPCR.

Vid de tidiga mätpunkterna erhölls för den råa (oxiderade) implantatytan ett högre genuttryck jämfört mot den släta (maskin) ytan för markörer ansvariga för att locka till sig mesenkymala stamceller (CXCR4) samt infästning av celler (integrin-β1). Vid de senare tidpunkterna uppvisade den oxiderade ytan ett högre genuttryck för benremodellerande gener, medan den släta implantatytan hade en högre inflammatorisk aktivitet. Dessa fynd var korrelerade med en större andel ben i kontakt med implantatet samt högre stabilitet för oxiderad yta och ett högre ratio för RANKL/OPG genuttryck. Den utvecklade protein-analysmetoden tillät analys av en stor mängd proteiner som utsöndras från odlade celler och indikerade interaktion mellan cellerna. I den kliniska studien visades att *Staphylococcus aureus* är den mest förekommande bakterien i hud hos patienter med benförankrade proteser. *S. aureus* associerades med ett uppreglerat genuttryck för TNF-α medan implantatförlust associerades med lägre genuttryck för IL-10 och osteocalcin.

Sammanfattningsvis presenterar denna avhandling en kombination av analytiska tekniker som möjliggör detaljerade studier av vad som händer på cellnivå vid gränsytan mellan implantat och vävnad, samt med avseende på benstruktur och stabilitet. Vi visade med denna plattform att ytstrukturen på implantat främjar cellulära signaler för att snabbt locka till sig celler och öka benbildningen vilket i sin tur ökar inläkning och stabilitet. Kandidat-faktorer såsom RANKL/OPG föreslås som en känslig indikator för att mäta graden av benbildning runt implantatet. I den kliniska studien ges indikationer på att specifika markörer (cytokiner) kan användas för att detektera förändringar runt implantaten och förutspå komplikationer.

LIST OF PAPERS

This thesis is based on the following studies, referred to in the text by their Roman numerals.

I. Omar O[*], Lennerås M[*], Svensson S, Suska F, Emanuelsson L, Hall J, Nannmark U, Thomsen P. Integrin and chemokine receptor gene expression in implant-adherent cells during early osseointegration. *J Mater Sci Mater Med*. 2010;21(3):969-80 [*]Equal contributions

II. Omar OM[*], Lennerås ME[*], Suska F, Emanuelsson L, Hall JM, Palmquist A, Thomsen P. The correlation between gene expression of proinflammatory markers and bone formation during osseointegration with titanium implants. *Biomaterials*. 2011;32(2):374-86. [*]Equal contributions

III. Lennerås M, Palmquist A, Norlindh B, Thomsen P, Omar O. Oxidized titanium implants enhance osseointegration via mechanisms involving RANK-RANKL regulation. *Clin Implant Dent Relat Res*. 2015;17 Suppl 2:e486-500. doi: 10.1111/cid.12276.

IV. Lennerås M, Ekström K, Vazirisani F, Shah FA, Junevik K, Thomsen P, Omar O. Adhesion and activation of monocytes and MSCs on titanium surfaces analysed by FACS, qPCR and protein profiling. *In manuscript*

V. Lennerås M[*], Tsikandylakis G[*], Trobos M, Omar O, Vazirisani F, Palmquist A, Berlin Ö, Brånemark R, Thomsen P. The clinical, radiological, microbiological and molecular profile of the skin-penetration site of transfemoral amputees treated with bone-anchored prostheses. *In manuscript.* [*]Equal contributions

Additional publications not included in this thesis:

- Omar O, Svensson S, Zoric N, Lennerås M, Suska F, Wigren S, Hall J, Nannmark U, Thomsen P. In vivo gene expression in response to anodically oxidized versus machined titanium implants. *J Biomed Mater Res A*. 2010;92(4):1552-66.
- Omar O, Suska F, Lennerås M, Zoric N, Svensson S, Hall J, Emanuelsson L, Nannmark U, Thomsen P. The influence of bone type on the gene expression in normal bone and at the bone-implant interface: experiments in animal model. *Clin Implant Dent Relat Res*. 2011;13(2):146-56.
- Slotte C, Lennerås M, Göthberg C, Suska F, Zoric N, Thomsen P, Nannmark U. Gene expression of inflammation and bone healing in peri-implant crevicular fluid after placement and loading of dental implants. A kinetic clinical pilot study using quantitative real-time PCR. *Clin Implant Dent Relat Res*. 2012;14(5):723-36.
- de Peppo GM, Palmquist A, Borchardt P, Lennerås M, Hyllner J, Snis A, Lausmaa J, Thomsen P, Karlsson C. Free-form-fabricated commercially pure Ti and Ti6Al4V porous scaffolds support the growth of human embryonic stem cell-derived mesodermal progenitors. *ScientificWorldJournal*. 2012;2012:646417.
- Elgali I, Igawa K, Palmquist A, Lennerås M, Xia W, Choi S, Chung UI, Omar O, Thomsen P. Molecular and structural patterns of bone regeneration in surgically created defects containing bone substitutes. *Biomaterials*. 2014;35(10): 3229-42.

CONTENTS

ABBREVIATIONS

AES	Auger electron spectroscopy
ALP	Alkaline phosphatase
AMAC-1	Alternative macrophage activation-associated CC chemokine-1
BMP-2	Bone morphogenetic protein-2
BA	Bone area
BIC	Bone-implant contact
CatK	Cathepsin K
CCL2/MCP-1	Chemokine (C-C motif) ligand 2/Monocyte chemoattractant protein-l
CXCR2/IL-8R	Chemokine (C-X-C motif) receptor 2/Interleukin-8 receptor
CXCR4/SDF-1R	Chemokine (C-X-C motif) receptor 4/Stromal derived factor-1 receptor
CXCL8/IL-8	Interleukin-8
CXCL12/SDF1	Stromal derived factor-1
CCL20	C-C motif chemokine ligand 20
CXCL5	C-X-C motif chemokine ligand 5
CXCL10	C-X-C motif chemokine ligand 10
CSF-1	Colony stimulating growth factor-1
ECM	Extracellular matrix
EDS	Energy dispersive X-ray spectroscopy

FACS	Fluorescence-activated cell sorting
FIB	Focused ion beam
HGF	Hepatocyte growth factor
IL-1β	Interleukin-1beta
IL-6	Interleukin-6
IL-10	Interleukin-10
LIF	Leukemia inhibitory factor
LPS	Lipopolysaccharide
M-CSF	Macrophage-colony stimulating factor
MIP-1α	Macrophage inflammatory protein-1 alpha
MMP	Matrix metalloproteinase
MSC	Mesenchymal stem cell
MCP-1	Monocyte chemoattractant protein
NPX	Normalised protein expression
OC	Osteocalcin
ON	Osteonectin
OPG	Osteoprotegerin
OPN	Osteopontin
PBMC	Peripheral blood mononuclear cell
PDGF	Platelet derived growth factor
PMN	Polymorphonuclear leukocytes

PS	Polystyrene
PEA	Proximity Extension Assay
PPAR-γ	Peroxisome proliferator-activated receptor-gamma
qPCR	Quantitative polymerase chain reaction
RANKL	Receptor activator of nuclear factor-kappa B ligand
RANK	Receptor activator of nuclear factor-kappa B
RSA	Roentgen stereo photogrammetric analysis
Runx2	Runt related transcription factor-2
SEM	Scanning electron microscopy
SPS	Skin-penetration site
TIMP	Tissue inhibitor of matrix metalloproteinase
TEM	Transmission electron microscopy
TGF-β	Transforming growth factor-beta
TNF-α	Tumor necrosis factor alpha
TNFR	Tumor necrosis factor receptor
TFA	Transfemoral amputation
TRAP	Tartrate-resistant acid phosphatase
VEGF-A	Vascular endothelial growth factor A
WB	Western blot
WNT	Wingless-type MMTV integration site family

1 INTRODUCTION

1.1 Introductory remarks

The global population is getting older and this is associated with an increased number of elderly people with increasing demands relating to their quality of life. One remarkable contribution to this challenge has been discovered and developed in Gothenburg by PI Brånemark and co-workers[1]. Since the discovery of osseointegrated implants in the late 1960s, the concept has been used for different reconstructive applications, including missing teeth and limbs, and for bone-anchored hearing aids.

Osseointegration is the biological process during which bone is formed directly on the implant surface without intervening fibrous tissue[1,2]. Over the years, and in parallel with the continuous introduction of new implant surface modifications, the main emphasis has been the morphology and mechanical strength of the bone-implant interface[3]. On the other hand, few studies have focused on the mechanisms of osseointegration *in vivo*, which entail the cellular and molecular events at the bone-implant interface. Furthermore, most of the recent research on the cellular and molecular events of osseointegration has been mainly exploratory and has related to the specific processes of bone healing (e.g. bone formation), whereas other major processes, such as the initial events of inflammation and the process of bone remodelling at the interface, have been largely neglected.

When it comes to the development of new generations of implants, it is fundamentally important to determine the effect of implant surface properties on the sequence of events, including the recruitment of different cells at the implant surface, the interactions of the different cells with the implant surface and the interactions of the interface cells with each other. Further, it is important that these cellular and molecular events are interrelated, not only to the degree of bone formation but also to the quality, composition and functional capacity of the bone formed at the interface.

There are several challenges for systematic studies that could provide detailed knowledge of the relationship between the cellular and molecular events *in vivo* and the structure, composition and biomechanical performance at the bone-implant interface. One major challenge is to employ a combination of tools and techniques for correlative analyses of these events at the interface. Most of the available cellular and molecular techniques are

well suited to *in-vitro* studies and several optimisations associated with the sample preparation and processing are needed in order to adapt these techniques to studies of the interface between bone and implant *in vivo*. In relation to this, another challenge is to obtain access to and apply appropriate sampling procedures to the narrow interface zone, where the actual events take place. In addition, the limited amount of biological material at the interface creates a substantial demand for techniques that could enable large-scale analyses of different biological factors and mediators.

The development of a methodological platform for studying the bone healing events at implants can also provide a new approach to evaluating and predicting tissue changes in relation to osseointegrated implants in a clinical setting. One clinical application of osseointegrated implants is the rehabilitation of patients with transfemoral amputations (TFA). In this procedure, there is a major challenge at the skin-penetration site (SPS), where an interface of titanium, bone and soft tissue comes into contact with the outer environment. Although the detection of bacteria and various symptoms and signs, such as redness, exudation and excessive granulation tissue, is common, the diagnosis of an infection at the SPS is still difficult. An increased knowledge of the cellular and bacteriological profile in relation to the clinical manifestations of the SPS is clearly needed.

1.2 Bone

Bone is a complex, dynamic and vascularised living tissue. It is a highly mineralised connective tissue with the main function of providing a framework that supports the body, anchors muscles and protects vital organs. It also acts as a reservoir for calcium and inorganic ions, a storage site for growth factors, as well as the site of the production of red and white blood cells[4].

Embryonically, bone is formed by two processes: endochondral and intramembranous ossification. These processes are also involved in fracture healing in the adult human[5]. Endochondral ossification starts with cartilage tissue being formed by chondrogenic cells from the mesenchymal cell lineage. The cartilage that forms is then mineralised and transformed into bone by osteoblasts. Intramembranous ossification, on the other hand, starts with mesenchymal condensation, which differentiates directly to osteoblasts, thereby forming bone.

1.2.1 Cellular components of bone

The bone microenvironment contains several types of cells, from those of mesenchymal origin to those of haematopoietic origin. The main components from mesenchymal origin are osteoprogenitors, pre-osteoblasts, osteoblasts, osteocytes and bone-lining cells. The haematopoietic cellular component consists of osteoclasts, tissue-resident macrophages and the precursors of different types of leukocytes residing in bone marrow niches[6].

Mesenchymal stem cells and osteoprogenitors

Mesenchymal stem cells **(**MSCs) are a diverse subset of multipotent precursors present in the stromal fraction of many adult tissues[7]. At the time of injury, MSCs are believed to be recruited from the surrounding tissues and the circulation, regulated by multiple factors[8]. MSCs have wide-ranging differentiation potential, meaning a capacity to differentiate into several cell types, including osteoblasts, chondrocytes and adipocytes. Several proteins are regulators of more than one of these differentiation pathways and there is cross-talk and cross-regulation between the different lineages. The differentiation processes and the signalling pathways that are involved have been extensively studied *in vitro*, but their identity *in vivo* is just starting to be uncovered[7]. The transcription factor, Runt related transcription factor-2 (Runx2), is a key marker of the commitment of MSCs towards the osteogenic lineage and excludes divergence towards other lineages[9]. One major and recently discussed aspect of MSCs relates to their immunomodulatory activities[10]. *In vitro*, MSCs have been shown, for example, to inhibit T-cell activation and immune-regulatory roles have also been documented *in vivo*[7]. Part of the explanation is thought to be the vast array of soluble mediators secreted by MSCs which are known to have immunomodulatory properties[7].

Upon receiving specific signals, such as bone morphogenetic protein-2 (BMP-2), MSCs commit to the osteogenic lineage, i.e. osteoprogenitors[11]. The osteoprogenitors have the properties of stem cells and thereby the potential to proliferate and differentiate[12]. The osteogenic differentiation process continues with the differentiation of bone progenitor cells into pre-osteoblasts, which then form mature osteoblasts. The mechanisms involved in the differentiation of MSCs into mature osteoblasts are complex and a variety of signalling molecules, including transforming growth factor-beta (TGF-β), BMPs and WNTs, are involved in this process[13].

Pre-osteoblasts and osteoblasts

The pre-osteoblast is a transitional stage between the proliferative osteoprogenitor and the mature osteoblast[11]. It has a low production capacity

for proteins and expresses a panel of early bone formation markers[14]. When pre-osteoblasts differentiate into osteoblasts, they become cuboid in shape and actively secrete the organic bone matrix. Osteoblasts firstly secrete the osteoid consisting of collagen and other proteins. During the early stage of bone formation, osteoblasts express high activity of alkaline phosphatase (ALP) enzyme, growth factors and molecules involved in auto- and paracrine regulations and cell-cell interactions. When the osteoid is mineralised, it develops into new bone tissue, which contains collagen type I, as well as non-collagenous proteins like osteopontin (OPN), bone sialoprotein (BSP) and osteocalcin (OC). During the process of bone matrix formation, osteoblasts extend cellular protrusions toward the osteoid seam and adhere to the existing matrix and neighbouring cells via integrins (mainly type β1).

Osteocytes

As bone is formed, osteoblasts are trapped within the matrix and become osteocytes. Osteocytes communicate with each other and with the blood vessels through narrow channels called canaliculi and they are able to transmit signals over long distances in the canalicular network. Osteocytes are believed to be the major mechanosensing cell type that responds to mechanical stimuli and controls the activity of osteoblasts and osteoclasts[15].

Osteoclasts

Osteoclasts originate from specific subsets of monocytes/macrophages of the haematopoietic lineage[6]. It is believed that osteoclast progenitors are recruited from haematopoietic tissues in the bone marrow to the site of bone resorption. They proliferate and differentiate into mononuclear pre-osteoclasts, which subsequently fuse with each other to form multinucleated osteoclasts[6]. Osteoclasts resorb the mineralised bone by making resorption pits. A number of key cytokines crucial for osteoclastogenesis and osteoclast development have been identified[16,17]. Macrophage-colony-stimulating factor (M-CSF) is believed to be of major importance for the proliferation of the osteoclast precursors. Receptor activator of nuclear factor-kappa B ligand (RANKL) is considered directly to control the differentiation process when binding to its receptor RANK on the osteoclast precursor surface[18]. Furthermore, osteoprotegerin (OPG), a member of the TNF-receptor family, is a major regulator of osteoclast differentiation and function[16]. OPG competes with RANK in binding to RANKL and acts as a break for osteoclasts. Furthermore, other cytokines and growth factors, such as tumour necrosis factor-alpha (TNF-α), interleukin-1beta (IL-1β), IL-6 and TGF-β1, have been shown to enhance osteoclastogenesis[16].

1.2.2 Structural components of bone

Bone exists in compact (cortical) or trabecular (cancellous) forms. Bone marrow resides in the spaces between the bone trabeculae and in the cavities of long bones and it contains multipotent stem cells. The main component of bone is a mineralised extracellular matrix (ECM) composed of inorganic and organic phases. The inorganic part consists primarily of plate-shaped carbonated hydroxyapatite, made of calcium and phosphate, as well as small amounts of other ions[19]. The organic phase is mainly type I collagen, in addition to proteoglycans and several non-collagenous proteins and growth factors[15].

The basic building block of bone is the structurally highly anisotropic mineralised collagen fibril and it is organised in concentric lamellae around a central blood vessel termed osteon. Each block is composed of alternating layers of plate-shaped crystals of the mineral, carbonated apatite, and layers of triple helical collagen molecules[20]. The presence of collagen is crucial for bone formation and bio-mineralisation, i.e. the nucleation and orientation of calcium phosphate crystals[21,22]. Several of the non-collagenous proteins, such as OC, BSP and osteonectin (ON), are also important for mineralisation[23].

1.3 Bone healing: inflammation, bone regeneration and bone remodelling

Bone healing is a complex process involving the co-ordinated participation of haematopoietic and immune cells, in conjunction with vascular and mesenchymal, skeletal, regenerative cells[8]. Multiple factors regulate the cascade of molecular events leading to the migration of cells, chemotaxis and the differentiation of the cells at the site of bone injury. Although simplified, the healing process can be divided into the closely linked phases of haematoma formation, acute inflammation, bone regeneration and remodelling.

1.3.1 Initial and early events of inflammation

When an injury occurs, the vasculature is damaged, with subsequent blood loss and the formation of a blood clot (haematoma). The blood clot acts as a substrate for haematopoietic cells that initiate the inflammatory cascade. Inflammatory cells are recruited to the site of injury and propagate the inflammatory response, which peaks after 24 hours and usually resolves within seven days[8]. Signalling molecules, such as TGF-β, platelet derived growth factor (PDGF), fibroblast growth factor (FGF) and vascular

endothelial growth factor (VEGF), are secreted and are important for angiogenesis and the recruitment of MSCs. The initial clot subsequently reorganises into a fibrin-rich granulation tissue[24].

During the early events of bone healing, the complex interactions of inflammatory cells and MSCs are controlled by multiple factors. These molecules can be roughly divided into cytokines, chemokines and integrins[8,25]. Further, several enzymes, which play a major role in the degradation of the fibrinous matrix and the early-formed granulation tissue, are secreted[26,27].

Inflammatory cytokines

Pro-inflammatory cytokines, such as TNF-α, IL-1β and IL-6, are secreted to a major extent by the early-recruited leukocytes, including polymorphonuclear leukocytes (PMNs) and monocytes/macrophages. These cytokines play a major role in activating the immune cells to clear insults, such as bacteria. Further, these cytokines are believed to be involved in triggering the subsequent events of extracellular matrix synthesis, stimulating angiogenesis and recruiting endogenous regenerative cells to the site of injury. The highest expression of these cytokines is seen within the first 24 hours after injury[8]. Normally, a downregulation is observed when woven bone is formed, followed by an increase during the active phase of bone remodelling. TNF-α promotes the recruitment of MSCs and stimulates osteoclastic functions[8]. Furthermore, although *in-vivo* studies have revealed crucial roles for TNF-α in bone regeneration, *in-vitro* studies have shown that this cytokine inhibits osteoblastic differentiation[25]. On the other hand, IL-6 is a pleiotropic cytokine, which influences several biological events in different organs including bone[28]. IL-6 performs both a pro-inflammatory and an anti-inflammatory role. In bone, although it is regarded as a pro-osteoclastogenic factor, IL-6 has been also suggested to play a role in osteoblast generation[29].

In addition to pro-inflammatory cytokines, leukocytes also secrete anti-inflammatory cytokines, such as IL-10. This is a key regulatory cytokine produced by a variety of cells, including activated macrophages, B-cells and regulatory T-cells[30]. IL-10 has been shown to inhibit the synthesis of pro-inflammatory cytokines, such as IL-1, IL-6, IL-8, TNF-α and IFN-γ[31], and it has been suggested to play a central role in limiting the immune response to pathogens, thereby preventing damage to the host tissue[32].

Chemokines and integrins

When the pro-inflammatory cytokines are activated, they generate a second wave of cytokines with the ability to induce chemotaxis in the nearby

responsive cells. Monocyte chemoattractant protein-1 (MCP-1/CCL2) is responsible for recruiting monocytes, memory T-cells and dendritic cells to sites of inflammation[33]. In bone, MCP-1 is also expressed and secreted by osteoblasts[34].

Interleukin 8 (IL-8/CXCL8) is a chemokine produced by macrophages and any cell with toll-like receptors that are involved in the innate immune response[35]. IL-8 is known as a main PMN chemotactic factor responsible for the migration of PMNs to the site of infection, induced after elevated levels of IL-1 and TNF-α[35].

Macrophage inflammatory protein-1 alpha (MIP-1α/CCL3) is a major factor in the recruitment and activation of PMNs during early inflammation. MIP-1α possesses high pro-inflammatory properties and may also play a role in regulating haematopoiesis[36]. MIP-1α has been shown to stimulate macrophage TNF-α, IL-1 and IL-6 production and has been suggested to play a role in modulating macrophage responses to inflammatory stimuli *in vivo*[37].

C-X-C motif chemokine 10 (CXCL10) is a chemokine that binds to the chemokine receptor, CXCR3, to induce chemotaxis, apoptosis and cell growth[38]. Alterations in CXCL10 expression levels have been associated with several inflammatory diseases[38]. CXCL10 has been shown to upregulate the expression of RANKL, which plays an important role in the formation of osteoclasts[38].

Stromal-derived factor-1 (SDF-1/CXCL12) is a growth-stimulating factor with several functions[39]. It binds exclusively to its receptor, CXCR4, and plays an important role in angiogenesis by recruiting endothelial progenitor cells from the bone marrow[40]. CXCR4 is expressed by haematopoietic leukocytes, especially neutrophils, and regulates their homing, retention and mobilisation[41]. Recently, it has been suggested that SDF-1 plays a critical role in the recruitment and function of MSCs during early bone healing and regeneration[42].

Integrins are transmembrane receptors crucial for interactions between cells, as well as between cells and extracellular matrix (ECM)[43]. Their function is primarily to regulate the cell cycle, cellular shape and mobility, thereby allowing rapid responses to events at the cell surface[43]. Integrins are believed to be expressed by every cell type and a cell may have several different types of integrin on its surface. Cells of the osteoblastic lineage predominantly express β1, α4, α5 αv[44], whereas αvβ3 complexes are more profound on

osteoclastic cells[44]. Leukocytes express at least 13 different integrins, among which β2 is a unique leukocyte-specific integrin[45].

Tissue-degrading enzymes

Matrix metalloproteinases (MMPs) play an important role in tissue remodelling associated with various physiological or pathological processes, such as angiogenesis and tissue repair. These enzymes are capable of degrading all kinds of ECM protein, as well as being involved in the cleavage of cell surface receptors and chemokine/cytokine inactivation[46]. Under normal physiological conditions, MMPs are precisely regulated at the level of transcription and by the inhibition of endogenous inhibitors (tissue inhibitors of metalloproteinases, TIMPs). When this regulation is interfered with, matrix metalloproteinase activity increases, leading to excessive tissue degradation and/or remodelling. One example is MMP8, which is mainly produced by PMNs[47,48] and is expressed at high levels during wound healing[49]. MMP-8 has also been implicated in several pathological conditions associated with chronic inflammation[49].

1.3.2 Osteogenic differentiation and bone regeneration

MSCs receive signals and biochemical stimuli from the surrounding microenvironment, as well as the neighbouring cells, which are likely to influence their differentiation into osteoprogenitors and osteoblasts,[14] termed *osteogenic differentiation*. Upon their osteogenic differentiation, MSCs express and release several factors, corresponding to the developmental stage of the osteoblastic cells and the ongoing activity during the healing cascade.

Alkaline phosphatase (ALP) is a group of enzymes with low substrate specificity, and is present in many human tissues, including bone, liver and white blood cells. ALP is responsible for phosphorylation and works effectively at an alkaline pH. During early bone formation, ALP is highly expressed and secreted and it is regarded as an early marker of osteogenic differentiation. The exact role of ALP is not known and several physiological functions have been suggested. They include the active transportation of substances across the membrane, an increase in the local concentration of inorganic phosphate and acting as a calcium binder[50]. Osteocalcin (OC) is believed to be exclusively produced by osteoblasts in bone and plays an important role in bone mineralisation[51]. OC represents a late marker during osteogenic differentiations of MSCs *in vitro* and bone formation *in vivo*[52].

Transforming growth factor beta (TGF-β) is a growth factor that controls many functions in most cells, such as proliferation and cellular differentiation. It exists in at least three isoforms, TGF-β1, 2 and 3, which are secreted by different cell types. Most leukocytes secrete TGFs and, during early fracture healing, it is believed that TGF-β1 is also secreted by platelets[53]. Further, TGF-β plays a major role in the recruitment and/or the differentiation of MSCs and osteoprogenitor cells[54]. TGF-β1 is also regarded as an anti-inflammatory mediator, and induces apoptosis in many cell types, such as inflammatory cells, through the SMAD pathway, for example[55].

Bone morphogenetic proteins (BMPs) belong to the TGF-β superfamily, and are potent pro-osteogenic factors with a capacity to induce bone formation throughout the body, including muscular and subcutaneous sites[56]. There are more than 25 different BMPs, with BMP-2, -6, -7 and -9 being the most potent ones in promoting MSC differentiation towards the osteoblastic lineage. BMP-2 exerts this effect by inducing the critical transcription factors, Runx2 and Osterix, via the SMAD pathway[57]. BMPs are mainly produced by osteoprogenitors, MSCs, osteoblasts and chondrocytes. Furthermore, haematopoietic cells have been suggested to be responsive to, and even produce, BMPs[58]. BMP-2 is regarded as a key-player in early bone healing and regeneration[59].

Runt-related transcription factor 2 (Runx2) is an osteoblast-specific transcription factor, essential for pluripotent mesenchymal cells to differentiate into osteoblasts[13]. The transcriptional control of Runx2 is required for the commitment of MSCs to the osteoblast lineage. It is well known that Runx2 is crucial for bone formation *in vivo* and Runx2 knock-out mice do not show any intramembranous or intracartilaginous bone formation[60].

1.3.3 Osteoclastic differentiation and bone remodelling

After early bone formation, the less organised heterogeneous woven bone undergoes gradual remodelling, where it is replaced by highly mineralised mature bone[24]. Bone remodelling also takes place as a continuous physiological process of coupled bone resorption and bone formation (homeostasis) and for the replacement of damaged bone[61]. During bone resorption, osteoclast precursors are recruited and subsequently differentiated at the site of bone resorption, where they express a variety of integrins. Osteoclasts express integrin-αvβ3 and also low levels of integrin-β2[62]. The binding of integrins forms a tight sealing zone of osteoclasts attached to the

bone surface. This makes bone resorption proceed by creating a highly acidic microcompartment, where the enzymatic degradation of organic components takes place. Lysosomal proteases, like cathepsin K (CatK), are also involved in this process. The subsequent process of bone formation begins once the osteoclasts leave the resorption pit. The mechanisms for this process are not fully understood, but it is possible that the release of growth factors from the dissolved matrix provides signals to osteoblasts to start forming bone[63,64].

Cathepsin K (CatK) is detected at the ruffled border membrane of osteoclasts and is thereby associated with the dissolution of the bone matrix[65]. It has the ability to catabolise elastin and collagen, leading to the degradation of bone and cartilage. The expression of CatK is stimulated by pro-inflammatory cytokines. Under normal conditions, tartrate-resistant acid phosphatases (TRAP) are highly expressed by osteoclasts and activated macrophages, but they are also expressed to some extent by osteoblasts and osteocytes[66].

The coupling between osteoblastic bone formation and osteoclastic bone resorption is a highly controlled process. The RANK/RANKL/OPG is a major coupling triad that has been well characterised and documented[18]. RANKL is a member of the TNF superfamily that appears to play an important role in both immune responses and bone morphogenesis[67,68]. Osteoblasts express RANKL as a membrane-associated factor. Osteoclast precursors that express RANK, a receptor for RANKL, recognise RANKL through the cell-cell interaction and differentiate into osteoclasts[16]. Osteoprotegerin (OPG), on the other hand, competitively binds to RANKL, preventing its pro-osteoclastic effects and thus controls and fine-tunes the remodelling process.

1.4 Material-tissue interactions in relation to osseointegration

The biological events leading to osseointegration resemble those of normal bone healing via the intramembranous route, i.e. direct bone formation without intermediate cartilage formation[69]. However, the presence of a bone-anchored implant, as well as the specific surface properties of such implants, are assumed to modulate the biological events. This will subsequently affect the degree of bone formation and maturation, implant integration and the biomechanical stability of the bone-implant interface[70].

In contrast to the late phases of osseointegration, the initial and early phases have not been well described *in vivo*. Most of the available knowledge on the

effect of titanium implants on the initial cellular and molecular activities has been obtained from soft tissue and *in-vitro* studies.

For instance, it has been shown *in vitro,* that the implant surface has a major influence on the initial events of protein adsorption, complement activation and thrombogenesis[71,72]. These processes are strongly linked to the subsequent processes of cell recruitment and differentiation, and disruption or dysregulation in these processes may lead to tissue damage or prolonged inflammation[73] or even the failure of the biomaterial[72].

With respect to the recruitment of cells, the early morphological studies of osseointegration demonstrated the recruitment of different cell types at the bone-implant interface preceding the process of bone formation[74,75]. MCP-1, a major chemotactic factor for monocytes/macrophages, has been shown *in vitro* to be highly expressed by human monocytes/macrophages in response to titanium particles[76]. Furthermore, other *in-vitro* studies have shown that the expression and/or release of MCP-1 and pro-inflammatory cytokines, e.g. TNF-α, is enhanced on micro-rough surfaces[77]. In contrast, surfaces with nano-topography reduce the expression of MCP-1, TNF-α and MIP-1α *in vitro*[78]. Further, MCP-1 has been found in granulomatous tissue surrounding loosened prosthetic implants and it may thus play a role in prolonged inflammation around biomaterials[76]. However, there is still lack of information on the expression of the major chemotactic factors at the bone-implant interface *in vivo* and the way this is related to the early organisation of tissue and bone formation at the bone-implant interface.

Similar to the effect on cell recruitment and the initial inflammatory response, the effect of titanium and titanium surface modification on integrin activities has been mainly studied *in vitro*[79-83]. For instance, an enhancing effect of surface roughness was found on the expression of integrin-β1 in MG63 osteoblasts and, by blocking the integrin-β1, (by gene-silencing), the osteoblastic secretion of ALP and OC was inhibited[84]. Another *in-vitro* study showed that blocking integrin-β1, by antibodies, inhibited the expression of BMP-2 in murine macrophages adhering to grit-blasted titanium surfaces *in vitro*[85].

Regarding osteogenic differentiation and bone formation activities, there is ample *in-vitro* evidence and several *in-vivo* studies show an influential effect of surface modification on the osteoblastic, bone-related, molecular activities. For instance, *in-vivo* studies have shown that grit-blasted and hydrofluoric acid-etched surfaces increase the expression of Runx2 and ALP in implant-adherent cells in the rat[86] and rabbit[87] tibiae compared with grit-blasted

titanium without acid etching. However, the way the temporal regulation of osteoblastic activities relates to the kinetic changes in terms of the amount of bone formation and implant stability at the bone-implant interface remains to be explored.

Despite being an integral component of bone, osteoclast and osteoclastic bone remodelling has not been sufficiently investigated at the cellular and molecular level *in vivo* in relation to osseointegration. Whereas bone remodelling is generally regarded as a late process at the interface[88] *in-vivo* morphological studies suggest that remodelling is an integral process which starts at an early stage after implantation[89]. *In-vivo* studies reveal the upregulation of the osteoclastic gene (TRAP) in response to titanium discs acid etched with a combination of hydrochloric and hydrofluoric acids compared with discs treated only with hydrochloric acid in the rabbit tibia after four weeks of healing[90]. Subsequent studies showed a positive correlation between osteoclastic gene expression (calcitonin receptor and TRAP) and the pull-out forces of the titanium discs in the rabbit tibia after four and eight weeks of healing[91]. Nevertheless, it remains to be elucidated how early the osteoclastic molecular activities are regulated by the implant surface properties. Moreover, given the highly controlled nature of the coupled bone formation and remodelling, exploring the molecular switches for bone remodelling, e.g. RANK/RANKL/OPG, with the emphasis on the role of the implant surface properties, is of great interest. One of the main aims of this thesis is to explore the relationship between the regulation of bone formation and remodelling activities at the implant surface *in vivo* and the development of the structure and ultrastructure of the bone in contact with the implant.

1.5 Challenges of osseointegration-based clinical applications

Based on the long-term success of osseointegration in dentistry, this concept was introduced to the orthopaedic field in 1990[92]. Patients with transfemoral amputations often experience problems related to the use of socket-suspension prostheses. With this treatment, instead of suspension through a socket, the prosthetic leg is directly anchored to the residual femur by an osseointegrated, percutaneous implant. Success has been shown both experimentally[93] and clinically[92,94-96], with reports of improved quality of life[92] and cumulative survival of 92% two years after surgery[92]. This treatment involves two operations, where the first stage is the surgical insertion of the fixture into the residual femoral bone, and it is then left

unloaded (usually for six months) in order to permit osseointegration[92]. During second-stage surgery, the abutment is inserted, penetrating through the skin into the implant and secured with a screw. A percutaneous implant protruding through the skin creates a breach of the skin barrier and constitutes a critical issue for these patients due to bacterial colonisation. A recent study showed frequent colonisation by *Staphylococcus aureus* and coagulase-negative staphylococci, known to be potentially virulent bacteria[97]. Whether deep infections arise from the superficial infections is not yet known and whether frequent bacterial colonisation can be coupled to fixture loosening requires further investigation.

A previous study validated a combined polymerase chain reaction and reverse line hybridisation protocol for identifying musculoskeletal infections[98]. The authors identified *S. aureus* as the most frequently found organism and they also reported that PCR-line blot hybridisation is more sensitive than routine culture. The same group also reported that 4-13% of total hip artroplasty revisions classified as aseptic are in fact low-grade infections, which are missed with routine diagnostics[99] although the diagnosis of infection did not have any obvious clinical consequences. For this reason, a knowledge of factors with a potential relationship to inflammation, microbial colonisation, infection and clinical manifestations of derangement, loosening or the failure of the biomaterial-tissue interface is urgently required.

1.6 Traditional methods for studying osseointegration

1.6.1 Light microscopy

This refers to the histological and morphological evaluation of tissue and cells in relation to the implant *in vivo* at the light microscopy level[74]. As a first step, samples are fixed, in order to maintain the cellular and structural integrity of the tissue, using different formulations of fixatives, such as formalin, that cross-link proteins and prevents enzymatic degradation. One of the most commonly used methods for morphological and histomorphometric analyses of bone-implant interface is performed on un-decalcified ground sections[100]. For histomorphometry, the percentage of bone in contact with the surface (bone-implant contact; BIC) as well as the percentage of bone area filling the thread (bone area; BA) are the most commonly studied parameters.

1.6.2 Electron microscopy

Electron microscopy provides possibilities to analyse structural details at higher level of resolution, compared to light microscopy. In the field of implants, scanning electron microscopy (SEM) has been commonly used to evaluate surface roughness and topography[101]. Transmission electron microscopy (TEM) uses the same basic principles as light microscopy, but electrons instead of light is used as a light source giving a thousand times higher resolution. This technique allow for visualisation of the micron- and sub-micron details of the tissue formed at the bone-implant interface. The difficulty to obtain intact and ultra-thin sections of the bone implant interface has been a major problem. However, the use of focused ion beam (FIB) milling and thinning, for subsequent TEM, has provided new insights on the ultrastructure and composition of intact bone-implant interfaces, down to the atomic level[102].

1.6.3 Biomechanics

The stability of an implant in bone is crucial for successful osseointegration and quantitative measurements can be made using several biomechanical techniques. Removal torque analysis is performed on rotationally symmetrical implants, measuring the force needed to loosen the implant under constant unscrewing rotation. It has been suggested that removal torque depends on the degree of implant integration in the recipient bone[103]. Push- and pull-out tests, on the other hand, appear to be fairly dependent on the quantity/quality of the surrounding bone[104]. In addition, implant stability has been measured using resonance frequency analysis (RFA). However, it is not yet clear what parameters are measured by RFA, i.e. the integration of the implant or the stiffness of bone surrounding the implant.

1.7 Cellular and molecular techniques with potential application to the bone-implant interface

1.7.1 Immunohistochemistry (IHC)

This technique refers to the process of detecting and visualising proteins intra- or extra-cellularly, by using antibodies that will bind specifically to antigens in the target protein/cell. The antibodies used for specific detection can be either polyclonal, which are a heterogeneous mix of antibodies that recognise several epitopes, or mono-clonal that show specificity for a single epitope. The primary antibody is subsequently visualised using secondary

antibodies with attached reporter molecules, such as fluorescent compounds, enzymes or metals, e.g. gold. The horseradish peroxidase (HRP) method is a commonly used approach. IHC has the major advantage of being able to show the spatial distribution of proteins and cells and is commonly performed on paraffin-embedded decalcified sections of bone. One drawback, however, is that the implant usually has to be removed and, as a result, the analysis is not actually performed on an intact bone-implant interface[105]. Further, there are limitations related to the semi-quantitative nature of the analysis, as well as the limitation when it comes to performing large-scale analyses of several factors.

1.7.2 *In situ* hybridisation

This technique permits analysis of the spatial distribution of expressed gene markers (RNA transcripts) of factors of interest, in tissue sections and in relation to biomaterials implanted in different tissues[106]. Using this technique, a labelled complementary DNA or RNA probe localises a specific RNA sequence in a tissue section. The target transcript is fixed, followed by hybridisation to the target sequence at elevated temperature. Only exact sequence matches should remain bound after the washing steps and the probe that was labelled with a radiolabel, antibody or fluorescent bases is visualised and quantified by autoradiography, immunohistochemistry or fluorescent microscopy. One major drawback of this technique is a low specificity, which can lead to a high false-positive rate. In spite of this, *in-situ* hybridisation has been valuable for the analysis of biomaterial-host interactions[107] and the key technique currently in use is fluorescence *in-situ* hybridisation, i.e. FISH[108].

1.7.3 Enzyme-linked immunosorbent assay (ELISA)

Another antibody-based analysis is ELISA, which involves at least one antibody with specificity for a particular antigen (protein). A primary antibody is coated on to a microtitre plate with the antigen-binding site(s) ready to catch antigens in the added sample. This bound antigen is subsequently recognised by an enzyme-conjugated secondary antibody to perform a “sandwich”. A substrate for the conjugated enzyme is added, thus initiating a colourimetric reaction and the absorbance is measured at 450 nm in a spectrophotometer. In relation to implants and biomaterials, the ELISA is a widely used technique *in vitro*, given its sensitivity and quantification potential. Furthermore, ELISA of selected factors has also been performed on clinically retrieved samples, such as crevicular fluid around teeth and implants[109,110]. One drawback in the field of biomaterials is the limited

amount of biological material in relation to the implant and the sensitivity when it comes to detecting protein secretions in very low abundance.

1.7.4 Western Blot (WB)

Western Blot is a semi-quantitative technique used to detect specific proteins in a sample of tissue homogenate or extract. Gel electrophoresis is used to separate native proteins by 3D structure or denatured proteins by the length of the polypeptide. The protein sample is transferred to a membrane where it can be detected by protein-specific antibodies. The antibodies are conjugated to an enzyme that, like the ELISA, catalyses a colour or fluorescence reaction that can be detected by a camera. WB has been used to provide important information on the presence of growth factors in implanted degradable biomaterials for bone regeneration[111,112]. However, some drawbacks exist, with difficulty in terms of background subtraction, saturation of signals and variation in blotting, which may interfere with accurate quantification.

1.7.5 Polymerase chain reaction (PCR)

PCR is based on the amplification of DNA molecule(s) to thousands and up to millions of copies of the starting template. In PCR, a heat-stable DNA polymerase assembles a new DNA strand using the single-stranded DNA as a template in the presence of DNA primers and the building blocks, deoxynucleoside triphosphates (dNTPs). When RNA is the target material, it is firstly reverse-transcribed into complementary DNA (cDNA). After PCR, the product can be transferred to an agarose gel in order to determine, semi-quantitatively, the relative amount of the starting genetic material. Today, quantitative PCR (qPCR) is the premier molecular enabling technology for the detection and quantification of nucleic acids and it is widely used both as a research tool and for many diagnostic applications. With its capacity to detect and measure critically low amounts of nucleic acids in a wide range of samples, together with its combination of speed, sensitivity and specificity, qPCR has become a gold standard for nucleic acid quantification.

1.7.6 Quantitative real-time PCR analysis (qPCR)

The qPCR reaction is initiated by combining the DNA (or cDNA) with a forward (sense) and reverse (antisense) primer pair in a reaction buffer containing equimolar ratios of four deoxynucleoside triphosphates (dNTPs), together with Mg^{2+}, a heat stable polymerase, (usually *Taq* polymerase) and a fluorescent DNA binding dye (or a probe). This mixture is heated to around 95°C which will separate the complementary DNA strands and allow primers to bind when the temperature is decreased. The mixture is rapidly cooled to

the annealing temperature of the primers (usually around 60°C), allowing them to find their complementary sequence and form a short double-stranded region. Primers must possess a free 3'-OH end to which an incoming dNTP is added by the *Taq* polymerase and the temperature is usually raised to 72°C, which is optimal for the polymerase. An intercalating dye, usually SYBR® Green, binds to all double-stranded DNA, giving a fluorescent signal that is proportional to the amount of DNA used for the quantification. Since the product of one cycle serves as the template for the next cycle, in theory, this results in the doubling of the amount of original template DNA present in the PCR solution. PCR thus leads to an exponential amplification of the initial DNA template, resulting in more than 1 x 10^6 copies of a homogeneous PCR product in 20 cycles[113].

Quality control

The addition of the reverse transcription step changes the nature of the qPCR assay and requires careful quality control of the RNA templates, as poor sample quality is a serious obstruction to completing a correct qPCR analysis[114]. However, when the quantity of RNA is very low, this might not be entirely possible. Nucleic acid concentration and purity can be determined spectrophotometrically, as the heterocyclic rings of the nucleotides absorb ultraviolet light at the absorption maxima around 260 nm for nucleic acids.

Purity is an important consideration for both DNA and RNA samples, as impurity leads to the inaccurate measurement of nucleic acid concentration. Genomic DNA (gDNA) not removed from the sample can also cause an increase in the estimate of copy number and it is therefore advisable to perform DNAse treatment on RNA samples. Further, impurity of the samples will cause the inhibition of the reverse transcription (RT) and/or the PCR. The most common inhibitors are carbohydrates and compounds used in the preparation of nucleic acids such as guanidine hydrochloride, EDTA, phenol and TRIzol®. As inhibitors are assay specific, inhibition will distort the results by leading to the loss of transcript proportionality. By simply diluting the sample, the problem with inhibitors can sometimes be solved. This can be further checked using a universal inhibition assay[115].

The integrity of the RNA can be assessed by a microfluidics-based device, which even provides an RNA integrity number (RIN). This system uses the 28S/18S ratio to measure the integrity of rRNA and aims to evaluate mRNA. The higher the RIN, the higher the quality of the RNA and the more likely it is that a sample will provide reliable data. In general, there are recommendations of a RIN ≥ 7 for subsequent qPCR analysis.

cDNA synthesis

To enable the analysis of gene expression with real-time PCR, the RNA has to be converted to complementary DNA (cDNA). The amount produced as cDNA reflects the input amounts of RNA, making reverse transcription (RT) a critical step for accurate quantification. The RT step contributes most of the introduced variation in experimental accuracy. To copy RNA to DNA, the enzyme, reverse transcriptase, needs a starting sequence, the primer, to initiate the synthesis. The main strategy for this is to use oligo(dT) sequences, random hexamer sequences or gene-specific primers. Random hexamer primers, i.e. short oligomers that are synthesised entirely randomly and will anneal throughout the target molecule, will copy all the RNA (tRNA, rRNA and mRNA). Oligo-dT primers bind to the poly(A)-tail of the mRNA, initiating transcription at the very end of the gene. It will produce long cDNAs, but it is sensitive to degradation. It has been shown that the efficiency of the RT reaction varies between different priming strategies, different RT enzymes and different genes, which makes it important to maintain consistency when analysing samples that should be compared[116].

Normalisation with reference genes

To be able to compare the gene expression between samples, differences in the amount of starting material need to be compensated for[117]. There are several options for this such as mass and volume, cell number or total RNA amount. However, it is not always possible to measure dry weight and cell number and total RNA is sometimes undetectable at very low concentrations. Furthermore, none of these approaches compensates for variations in RNA quality, RT or PCR inhibition. The use of one or more stable reference genes is crucial for the correct interpretation of qPCR data. No universal reference gene exists and the stability of the reference gene(s) should be validated for each individual study. In this thesis, the relative gene expression was evaluated using the $2^{-\Delta\Delta Cq}$ method[118].

Primer design and validation

Primer design and validation is a key factor for successful PCR[119]. Physical parameters, such as the base composition and concentration of primers, affect PCR efficiency and sensitivity. Primers should have between 18-24 bases, a 40-60% G/C content and a balanced distribution of G/C and A/T bases. At a melting temperature (Tm) of 55-65°C the annealing occurs without an internal secondary structure (e.g. hair-pin) formation. Further, primer pairs should have similar melting temperatures (within 2-3°C) and no significant complementarity (> 2-3 base pairs), particularly not at the 3'-ends. It is important always to test the primers in the "wet lab" before using them. This validation procedure is performed by checking the specificity (by melt curve

and on gel electrophoresis), reproducibility (C_q values) and PCR efficiency (by standard curve). This can be followed by the application of specific tests as the limit of detection (LOD) and limit of quantification (LOQ).

MIQE guidelines

The practical simplicity of qPCR, together with the opportunity to detect a single molecule in a wide range of samples, has resulted in an exceptional number of publications reporting qPCR data, all with different reagents, protocols and analysis methods. There is therefore a need for guidelines when publishing data from this widely used technology. The MIQE guidelines: Minimum Information for Publication of Quantitative Real-Time PCR Experiments, aim to help produce data that are more uniform, more comparable and ultimately more reliable[114].

1.7.7 Proximity extension assay (PEA)

This is a recently developed protein-profiling method consisting of a multiplex assay, which simultaneously measures 92 proteins in as little as 1 µl of supernatant. The technique is based on a pair of oligonucleotide-labelled antibodies that are allowed to bind pairwise to the target protein in the sample. When the two probes are in close proximity, a new PCR target sequence is formed and subsequently quantified using qPCR. Each antibody pair contains a unique DNA sequence allowing hybridisation only to each other and only matched DNA reporter pairs are amplified with real-time PCR. One major advantage of this technique is that a critically low amount can be measured in small biological material. This technique has been used for the detection of low-abundance proteins in human blood but not as yet in the field of biomaterials[120,121].

1.7.8 Flow cytometry

Flow cytometry is a technique that analyses cells under flow. The method is based on specific light scattering: forward scatter (FSC), which measures the relative size of the cells, and side scatter (SSC), which measures the granularity or inner complexity. Flow cytometry can be used to count the cells/particles in suspension, separating live/dead cells and for immune phenotyping. Modern instruments are able to analyse several thousands of particles every second in “real time” and are able actively to separate and isolate particles with specified properties. Fluorescence-activated cell sorting (FACS) is a specialised type of flow cytometry providing the option of sorting a heterogeneous mixture of cells, one at a time, to a new tube for downstream applications. It is based upon the specific light-scattering and fluorescent characteristics of each cell. A wide range of fluorophores can be

used to label the cells and they are usually attached to an antibody that recognises a target feature on or inside the cell. Flow cytometry is an automated method that makes it possible to objectively measure the features of single cells in suspension with many parameters. One drawback is the limitation of available antibodies for species other than humans and mice.

Flow cytometry is a powerful technique for analysing inflammatory exudates and large differences in cellular responses to different biomaterials *in vivo* have been observed using this technique[122]. A recent study used flow cytometry to identify specific markers indicative of septic and aseptic loosening in patients with total hip arthroplasty and suggested flow cytometry as a diagnostic tool[123].

2 AIM

The main objective of this PhD thesis was to develop a methodological platform, allowing for detailed analyses of cellular, molecular and structural events at the bone-implant interface, in order to advance our understanding of the mechanisms of osseointegration.

2.1 Specific aims of the included studies

I. To investigate the early gene expression denoting cell recruitment, cell adhesion and initial inflammation in cells adhering to different titanium implants *in vivo* and to relate these activities to the initial tissue organisation and cell distribution at the bone-implant interface

II. To investigate gene expression crucial for inflammation, bone formation and remodelling at different titanium implants up to 28 days *in vivo* and to correlate the molecular activities with the biomechanical capacity of the bone-implant interface

III. To investigate the kinetic changes in the structure and ultrastructure of bone interfaces with different titanium implants *in vivo* and to relate these events to the regulation of remodelling activity at the bone-implant interface

IV. To investigate the cell-specific molecular activities of human monocytes and MSCs adhering to different titanium implants in single- and co-culture systems and to evaluate the protein secretory profile of the implant-adherent cells, separately and in co-cultures with direct cell-cell contact

V. To determine the frequency of macroscopic signs of inflammation in patients with transfemoral amputations treated with osseointegrated fixtures and percutaneous abutments, and to employ the qPCR technique for correlative analyses between gene expression in the abutment-adherent cells and clinical, radiological and microbiological findings

3 MATERIALS AND METHODS

3.1 Implants (Paper I-IV) and abutments (Paper V)

In the experimental (*in-vivo* and *in-vitro*) studies (Paper I-IV), screw-shaped titanium implants, 2 mm in diameter and 2.3 mm in length, were used. Two different surfaces were selected, machined and anodically oxidised (TiUnite^{TM}), All implants were manufactured and sterilised by Nobel Biocare, Göteborg, Sweden.
In the human clinical study (Paper V), commercially available components from Integrum AB (Mölndal, Sweden) were used. In this study only the abutment was used for analysis. It has a diameter of 11 mm and length between 72-77 mm. The human abutments were either machined titanium (cp-Ti grade IV) (n=29) or titanium alloy (Ti6Al4V, grade V) (n=1). The abutments were cleaned by ultrasonication followed by sterilisation by the manufacturer.

3.2 Surface characterisation

The material surfaces of the implants in the experimental studies (Paper I-IV) were characterised, both qualitatively and quantitatively, using chemical and topographical techniques as outlined below. In the clinical study (Paper V), the surface morphology of the abutment was evaluated using scanning electron microscopy.

3.2.1 Profilometry

Topographical analysis of machined and oxidised implant surfaces (n=3) was performed using non-contact 3D interference microscopy (WYKO NT-9100). The measurements were performed on a 125 x 95 μm area on flanks, tops and valleys of two nonadjacent threads on each implant type. The following surface parameters were derived: S_a (arithmetic mean of the absolute values of deviation from a mean plane), S_t (peak-to-valley distance) and S_{dr} (developed interfacial area ratio). Similar information was provided by analysing the surface of one abutment in Paper V.

3.2.2 Auger electron spectroscopy

The top atomic layers of the machined and oxidised implant surfaces were analysed by Auger electron spectroscopy (AES PHI 660 scanning Auger

microscope) (n=3) in order to evaluate the chemical composition of the implant surfaces. The analysis was made on the thread top and valley of the implant over 30 x 30µm analysis area. The implants were analysed either as-received or after short cleaning with argon ion.

The oxide thickness of one oxidised implant was determined by AES in combination with argon ion sputtering. The depth profiling was conducted on the top of the third thread using Ar^+ ion gun and the thickness of the titanium oxide layer was calculated.

3.2.3 Transmission electron microscopy

Ultrathin sections for TEM analysis were prepared from one implant of each type using focused ion beam (FIB) microscopy. The implants were embedded in LR White plastic resin and cut longitudinally into two halves. The exposed side of the implant was sputter-coated with a thin film of palladium (Pd), mounted on stubs and placed in the focused ion beam (FIB) microscope (FEI Strata DB235, FEI Company, Eindhoven, Netherlands). Ultrathin sections (100 nm) were prepared for TEM. Bright field and dark field imaging, selected area electron diffraction analysis (SAED) and energy dispersive X-ray spectroscopy (EDS) were performed.

3.2.4 Scanning electron microscopy

Four abutments (one new in sterile packaging, and three re-cleaned after retrieval) were evaluated in terms of surface morphology. Imaging was performed in secondary electron mode in a Leo Ultra 55 FEG-SEM (Zeiss) operating at 10 kV, using magnification levels up to x200 000. Different locations on the abutment were evaluated while the major focus was on the zone of the bone canal (1.5-3.5 cm from the proximal hexagonal end).

3.3 Study design

The present thesis was performed *in vivo* (animal), *in vitro* (cell culture) and in human.

3.3.1 Animal model and surgical procedure (Paper I-III)

Sprague–Dawley rats (200-250g) were used for implantation of titanium implants. After shaving and cleaning (5 mg/mL chlorhexidine in 70% ethanol), the medial aspect of the proximal tibia metaphysis was exposed. Implant installation sites were prepared with Ø1.4 and 1.8 mm round burs

under profuse irrigation with NaCl 0.9%. Each rat received two oxidised implants in one tibia and two machined implants in the opposite tibia. After different time points of implantation (3h-28d), the rats were sacrificed using an intraperitoneal overdose of sodium pentobarbital (60 mg/mL). The samples were retrieved depending on the subsequent analyses.

For gene expression analysis implant with the adherent cells were retrieved by unscrewing and immediately preserved in RNA*later* (Paper I-III). Furthermore (in Paper II), removal torque was measured on the implants prior to preservation for gene expression analysis. In addition, the peri-implant bone was retrieved using a trephine with internal Ø 2.3 mm and immediately preserved in RNA*later* (Paper II).

For immunohistochemistry, histology, histomorphometry and ultra-structural analyses: implants with the surrounding bone were dissected *en bloc* and subsequently fixed in formaldehyde (4%).

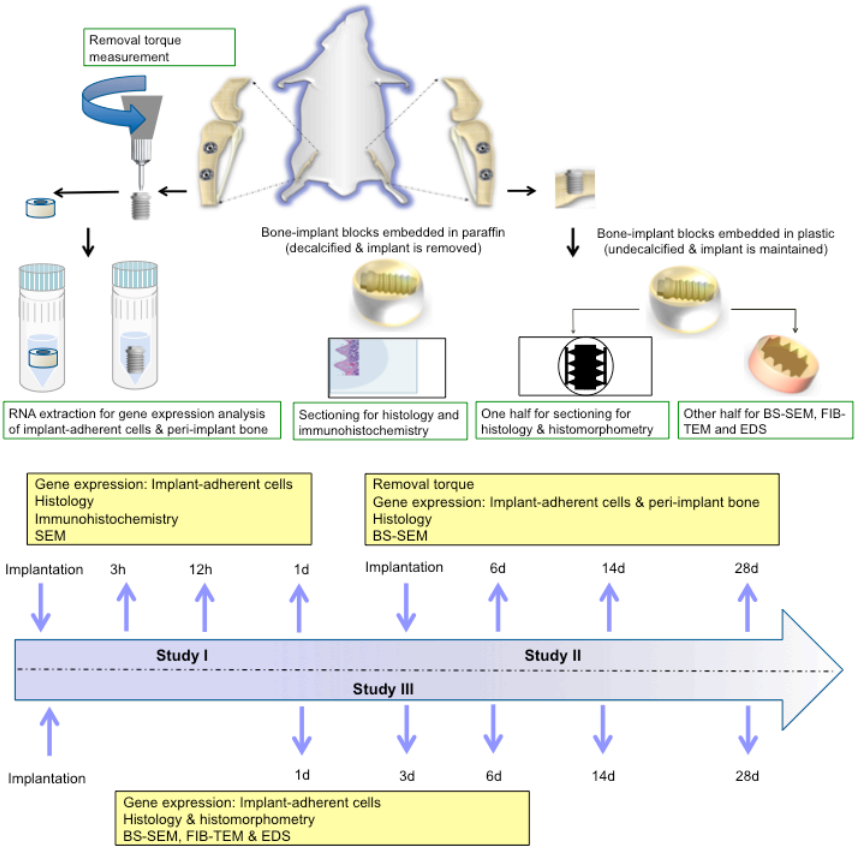

Figure 1: Experimental design for studies I, II and III.

3.3.2 In vitro model using mono- and co-cultures (Paper IV)

For the *in vitro* study, monocytes and MSCs were cultured on polystyrene (PS), machined titanium (Ma) and anodically oxidised titanium (Ox) implants. The screw-shaped implants were pooled with 3 implants in each well. Monocytes were isolated from human blood using a two-step separation procedure, where the monocytes were isolated from the peripheral blood mononuclear cells (PBMCs) by negative isolation. The human MSCs were commercially available adipose-derived cells expanded without adding osteogenic factors. Human monocytes and MSCs were stained with Vybrant DiO (yellow) and DiD (blue) cell-labelling dyes. The stained monocytes and MSCs were seeded on the polystyrene (PS) and on screw-shaped machined (Ma) and oxidised (Ox) titanium implants. The cells were seeded as separate mono-culture or co-cultures (1:1) of 1×10^5 monocytes and 1×10^5 MSCs in 96-well plates. After 24h, culture media was collected from each experimental group and stored (at-20°C) for subsequent ELISA and protein profiling analyses. At the same time, the pooled implants were transferred, with the adherent cells, to a new well with new culture media and placed in the incubator for additional 1h period. Supernatant from the 1h culture of implant-adherent cells was collected and stored for protein profiling. The implant-adherent cells were detached from the titanium implants and the polystyrene surface using trypsin. The detached cells were counted and prepared for FACS and subsequent qPCR (gene expression) analyses.

3.3.3 Human clinical study (Paper V)

During a two-year period thirty consecutive patients with transfemoral amputation treated with bone-anchored prostheses were enrolled in the study. The reasons for abutment exchange/removal were either mechanical failure or infectious problems. Three of these patients had their abutments removed due to fixture loosening as part of complete removal of the implant system. The abutment exchange or removal was performed in the operation theatre under sterile conditions. The clinical appearance of the skin penetration site (SPS) was documented by photographs and macroscopically for skin colour, exudation and presence of granulation tissue. Swabs for microbiology were taken from three different compartments: the SPS, a defined area of the abutment surface as well as inside the bone canal. The removed abutment was placed in a tube containing RNA*later*® for subsequent gene expression and Western blot analyses.

3.4 Analytical procedures

In the present thesis, combinations of different cellular, molecular, morphological, ultrastructural and functional techniques were used in the respective studies. In addition, microbiological analysis was performed on bacterial swabs at routine microbiology laboratory at Sahlgrenska University Hospital.

3.4.1 Gene expression analysis (Paper I-V)

In Paper I-III total RNA was extracted using Qiagen RNeasy Micro kit (implant-adherent cells) and Mini kit (peri-implant bone). Prior to isolation the samples were placed in lysis buffer (RLT buffer + β mercaptoethanol for implant-adherent cells and QIAzol + steel bead for peri-implant bone) and homogenised in Tissuelyser.

In Paper IV, RNA was isolated from FACS-sorted implant-adherent cells. The cells were sorted directly into a 96-wellplate with 5µL lysis buffer (Cellulyser) in each well.

In Paper V, total RNA and protein was extracted from the abutment-adherent cells using a combination kit from Macherey-Nagel. Prior to extraction the abutment was placed in RP1 lysis buffer (only covering the part that had been in the bone canal) and roughly vortexed for 3 minutes, thereby homogenising the adherent cells.

The concentration and purity of RNA was measured, when applicable, using a nanospectrophotometer (NanoDrop, Thermo Scientific) and the quality of RNA samples was evaluated by chip electrophoresis in an Agilent 2100 Bioanalyser (Agilent Technologies).

In Paper I-III, mRNA was transcribed to cDNA using iScript cDNA synthesis-kit (Bio-Rad Laboratories) and in paper IV and V Grandscript cDNA synthesis kit (TATAA Biocenter AB) was used. Primer design was performed using the Primer3 web-based software or Primer Blast (http://www.ncbi.nlm.nih.gov/tools/primer-blast)[124]. Primers were designed to yield short amplicons and the efficiency and specificity of the assays were confirmed.

In Paper I-III, quantities of target genes were normalised using the expression of 18S ribosomal RNA (18S).

In Paper IV, the gene expression was normalised to the number of sorted cells (200 FACS-sorted cells). In Paper V, the samples were screened for a reference gene panel (TATAA Human reference gene panel) for determining the most stable reference gene(s). Hence, a mean of 18S, GAPDH and YWHAZ was used for normalisation.

The normalised relative quantities were calculated using the delta-delta Cq method and assuming 90% PCR efficiency ($k*1.9^{\Delta\Delta Cq}$).

3.4.2 Flow cytometry (paper IV)

Prior to flow cytometry, cells were detached from the implants by trypsin, counted on Nucleocounter and re-suspended in FACS buffer. The flow cytometry analysis was carried out on FACS Aria flow cytometer (BD Bioscience). Cells were acquired using forward scatter (FSC) and side scatter (SSC) in combination with the cell stains DiD and DiO (Thermo Scientific) to distinguish monocytes and MSCs in the co-culture. A total of 200 monocytes and MSCs, respectively, were sorted into a 96-well plate for qPCR. After lysis, the plate was stored (at -80°C) for subsequent qPCR analysis (as described above). The acquired flow cytometry data was analysed by FlowJo Version 9.3.2 software (TreeStar).

3.4.3 Enzyme-linked immunosorbent assay (Paper IV)

In the *in vitro* study (Paper IV), the levels of secreted TNF-α and BMP-2 were analysed using sandwich ELISA (R&D systems) according to the manufacturer's instructions. Briefly, the plate was coated with a capture antibody over night, after which the supernatant was added to the wells. The absorbance was measured at 450 nm using a microtiter plate reader (SPECTRAmax PLUS, Molecular Devices).

3.4.4 Protein profiling (Paper IV)

In the *in vitro* study (Paper IV), large-scale protein analysis was performed on the supernatants using Proseek Multiplex Inflammation 96x96 kit (Olink Bioscience). Ninety-two proteins (and 4 controls) were simultaneously measured in the supernatant by real-time polymerase chain reaction using the BioMark HD (Fluidigm). Details about the procedure are at Olink webpage (http://www.olink.com/products/proseek-multiplex/downloads/data-packages). Briefly, the 96 antibody probe pairs were allowed to bind to their target proteins in the samples. An incubation mix was prepared, which contains: A-probes (96 antibody probes labelled with A oligos), B-probes (96 antibody probes labelled with B oligos), incubation solution and stabiliser.

Three microliters of the incubation mix was added to each well in a 96-well plate together with 1 µL of each sample, and incubated at 4°C over night. Thereafter, 96 µL of an extension mix was added to each well of the *incubation plate*. Extension was performed on T100 thermocycler (Bio-Rad Laboratories) using a thermal cycling protocol. After the pre-amplification, 7.2 µL of a detection mix was transferred to a new 96-well plate (*Sample plate*) and mixed with 2.8 µL from the *Incubation plate*. Additional plate containing the individual primers (*Primer Plate*) was unsealed.

From the Primer Plate, 5 µL was transferred to the 96x96 Dynamic Array on the BioMark platform (Fluidigm). To the same chip (separate wells), 5 µL from each well in the *Sample Plate* was transferred and a thermal cycling protocol was applied. The quality control of the data was checked in the Fluidigm Real-Time PCR Analysis Software. The raw data was imported to the Excel QC sheet to control the samples against the internal controls. The normalisation was performed according to the formula NPX = Correction factor – $ddCq_{analyte}$ where NPX (Normalised protein expression) are log2-transformed values, with a low value corresponding to low protein levels.

3.4.5 Western blot (Paper V)

In Paper V, cellular proteins from the abutments were isolated with NucleoSpin RNA/protein kit (Macherey-Nagel) according to the manufacturer's instructions. The protein concentration was determined using a Pierce®BCA protein Assay kit (Thermo Scientific). Equal amounts of proteins were loaded per well and separated on a gel and transferred to Nitrocellulose membranes (Bio-Rad Laboratories). To prevent non-specific binding, membranes were blocked with 2% non-fat milk powder in Tris-buffered saline. The membranes were incubated with HRP-conjugated ProteinA antibody (Abcam). The membranes were washed and developed using chemiluminescence detection kit (Bio-Rad Laboratories). Digital detection was made using the Gel imaging system, supplied with Image Lab Software (Bio-Rad Laboratories).

3.4.6 Bacterial culture (Paper V)

In Paper V, patient samples were taken for bacterial culture with a sterile cotton swab, transported in a coal-based medium and cultured according to a routine procedure (Clinical Microbiology Lab, Sahlgrenska University Hospital). Briefly, swabs were streaked on 5 different agar plates: Columbia horse blood (incubated under aerobic and anaerobic conditions), Grand Lux plate, *Streptococcus* plate, Chromogenic *Staphylococcus* plate and Drigalski plate, following incubation at 37°C from 2 to 6 days. The swabs were

enriched in order to increase the detection and incubated for 6d at 37°C. All cultures were analysed by experienced microbiological analysts.

3.4.7 Immunohistochemistry (paper I)

The bone-implant specimens were fixed in modified Karnovsky's media for 2h, decalcified in 10% EDTA for 10d and embedded in paraffin. While the paraffin was still in the molten stage, the implants were unscrewed and the embedding procedure was continued. Finally, 4 µm thick sections were produced, mounted on poly-L-lysine slides (Menzel GmbH). The sections were deparaffinised, hydrated and incubated with primary antibodies CD163 (Santa Cruz Biotechnology), a marker for monocyte/macrophage cells, and periostin (Abcam), a marker for mesenchymal stem cells and osteoprogenitors. Negative control slides were prepared by omission of the primary antibody and incubation with 1% BSA in PBS. In addition, 10 µm thick sections were produced, mounted on regular glass slides and stained with hematoxylin and eosin. Qualitative analyses were performed under light microscopy (Nikon Eclipse E600).

3.5 Histology (Papers I-III) and histomorphometry (Paper III)

The implant-bone specimens were fixed in formaldehyde and subsequently dehydrated in a graded series of ethanol. The specimens were embedded in plastic resin (LR White). The embedded specimens were divided along the long axis of the implant using a diamond saw. One half was used for histological and histomorphometric analyses, and the other half was used for qualitative backscattered scanning electron microscopy and ultrastructural analyses (see below). A central ground section with a final thickness of 10–20 µm was obtained and stained with 1% toluidine blue. The qualitative histological evaluation was made with an optical microscope using ACT-1 imaging software (Nikon).

Quantitative histomorphometry was performed with the optical microscope and using Easy Image Measurement 2000 analytical software (Technooptik AB). The amount of bone between the implant threads (bone area percentage, BA%) was measured as well as the amount of bone in direct contact with the implant surface (bone-to-implant contact percentage, BIC%).

3.5.1 Scanning electron microscopy (Paper I-V)

SEM was performed on different types of specimens.

In Paper I and IV, the analysis was performed on the unscrewed implants, *in vivo*, and cultured implants, *in vitro*, to evaluate tissue and/or cells adherent to the implant. After fixation with modified Karnovsky's medium, the retrieved implants were rinsed with sodium cacodylate buffer and impregnated with osmium using a modified osmium-thiocarbohydrazide-osmium technique (OTOTO). The specimens were then dehydrated in ethanol, dried and mounted on SEM stubs. All specimens were examined in a Zeiss DSM 982 Gemini SEM (Paper I) and Leo Ultra 55 FEG SEM (Paper IV).

In Paper II and III, the backscatter-SEM analysis was performed on the second half of the resin-embedded bone-implant specimens. The specimens were polished and sputter-coated with Au/Pd prior to mounting in the microscope chamber. Imaging was performed in the backscattered electron mode using high acceleration voltages in Leo Ultra 55 FEG SEM (Paper II and III) and Leo 440 LaB6 SEM (Paper III). Elemental analysis (Paper III) using energy-dispersive X-ray spectroscopy (EDS) was also performed.

3.5.2 Transmission electron microscopy (Paper III)

After BS-SEM, selected samples were transferred to a focused ion beam microscope (FEI Strata235) for preparing cross-sections for transmission electron microscopy (TEM) analysis. Ultrathin sections (100 nm thick containing both implant material and tissue) were prepared. Analysis of the TEM samples was performed in a FEI Technai F20 TEM operating in the high-angle annular dark field scanning transmission electron microscopy (HAADF-STEM) mode for optimal contrast between the implant and bone tissue. In addition, site-specific elemental analysis was performed using a nanoprobe and energy-dispersive X-ray spectroscopy (EDS).

3.6 Removal torque analysis (paper II)

In paper II, and immediately after sacrificing the rats, torque analysis was performed on the implants *in situ*. The implants were exposed and a special hexagonal screw-driver, connected to the torque instrument, was fitted into the implant internal hexagon. The torque was registered versus the rotation angle and followed in real time. After the breakpoint was reached, the procedure was continued under the constant rotation to determine deformation curve. After recording the torque values, the implant was completely unscrewed and preserved for gene expression analysis (as described above).

3.7 Scoring system (paper V)

In Paper V, in order to clinically describe the SPS, a classification system was constructed. The commonly used Holgers scoring system for the assessment of soft tissue conditions around bone-anchored hearing aids served as a starting point. Due to major anatomical and technical differences, a modified classification system was created, taking the following clinical signs into account: Skin colour (normal=0, purple=1, red=2), presence of exudate (no exudate=0, serous=1, purulent=2), presence of granulation ring (0/1) and presence of fistulas (0/1). With this system a perfectly normal SPS without any signs of soft tissue irritation is classified as score 0, whereas a SPS with redness, purulent secretion, granulation ring and fistulas would receive a maximum score of 6.

3.8 Statistical analyses

In the present thesis, different statistical analyses were performed depending on the research questions.
In Paper I and II, Wilcoxon signed rank test was used to analyse the differences in the gene expression levels between the two implant types, at each specific time point. For comparing the gene expression between the different time points, for each implant type, one-way ANOVA was used. Topographical, chemical and torque measurement comparisons were performed using one-way ANOVA followed by Bonferroni's *post hoc* test.

In Paper III, Kruskal-Wallis test and/or Mann-Whitney test were used to analyse differences between the two implant types or between the different time points with respect to histomorphometry and gene expression.

In Paper IV, statistical comparisons were made between the different experimental groups, comparing the 3 analysed surfaces, mono-cultures versus co-cultures and between the two cell types. For cell counting and ELISA, one-way ANOVA and *post hoc* LSD test, were used. For gene expression and protein profiling analyses, one-way ANOVA was performed with Bonferroni correction, considering the multiple analysed factors.

In addition, correlation analyses were performed, when applicable, in the different studies. In Paper II, Pearson correlation analysis was performed between removal torque values and the expression levels of different analysed genes. In Paper III, Spearman correlation analysis was performed to determine correlations between the analysed genes. In Paper V, Spearman

correlation analysis was performed between the different clinical, radiological, microbiological and gene expression parameters.
All analyses were performed in IBM SPSS® Statistic software and *p*-values of <0.05 were considered statistically significant.

3.9 Ethical approval

Animal studies (Paper I-III)
The animal experiments were approved by the University of Gothenburg Local Ethical Committee for Laboratory Animals (Dnr 306-2006 and 301-2009).
Human clinical study (Paper V)
The transfemoral abutments were obtained from patients undergoing surgical exchange of abutments at the *Centre of Orthopaedic Osseointegration, Sahlgrenska University Hospital (Mölndal), Sweden*. Written consent was obtained from all patients. The consent form was part of the ethical application and was approved together with the study protocol by the Regional Ethical Review Board of Gothenburg (Dnr 110-14).

4 RESULTS IN SUMMARY

Paper I

The first study was performed to investigate the expression of pro-inflammatory cytokines, chemokines and adhesion markers during the first 24h of implantation.

With respect to chemokines and chemokine receptors, for both machined and oxidised implants, IL-8R expression showed a temporal increase from 3h to 12h, followed by a decrease thereafter. No difference in the IL-8R expression level was found between the two surfaces at any of the evaluation time periods. The expression of MCP-1 at the oxidised implant peaked at 12h and decreased thereafter, whereas at the machined implants MCP-1 showed a continuous temporal increase up to 24h. On the other hand, the expression of chemokine receptor CXCR4 showed 11-fold up-regulation at the oxidised surfaces compared to the machined after 12h of implantation.
With respect to the pro-inflammatory cytokines, the machined implant was associated with higher expression of TNF-α (2-fold) and IL-1β (3-fold) compared to the oxidised implant, at 3h and 24h, respectively. Both cytokine expression levels continuously increased with time at the machined surface. Regarding the integrin gene expression, and irrespective of the implant type, the temporal pattern for all analysed integrins peaked at 12h, except for integrin-αv where the peak appeared after 24h. Comparing the two implant surfaces, oxidised implants revealed higher expression of integrin-αv (at 12h), integrin- β1 (at 24h) and integrin-β2 (at 12h and 24h).

Histological analysis showed a rapid organisation of the early-formed haematoma in the threads of the implants. Immunohistochemical analysis revealed that both CD163-positive monocytes/macrophages and periostin-positive osteoprogenitors were present in the newly formed haematoma. Furthermore, a prominent finding was the fibrin-like strands running parallel to the machined but not the oxidised surface.

SEM showed a high proportion of fibrinous material adherent to the machined implants but not to the oxidised. Numerous erythrocytes and leukocytes were captured within the fibrin and smaller cells were also visible on the machined surface. An interesting observation was that several relatively large mesenchymal-like cells, were evident at the oxidised implant surface. These cells revealed a firm anchorage by extending their processes onto surface features of the oxidised implant.

Paper II

In the second study, the material surface-induced gene expression at 6, 14 and 28d were evaluated and related to the biomechanical assessment of the strength of the bone-implant interface.

In comparison to the machined implants, higher removal torque values were recorded for the oxidised implants at all time periods with increases (at breakpoint) of 140%, 170% and 190%, after 6, 14, and 28d, respectively. However, at 6d the difference was not statistically significant. Furthermore, the two implant types demonstrated two distinctly different deformation curves. For the machined implant, the deformation curve showed a linear torque increase up to few degrees, reaching a plateau at constant or slightly increasing torque with the increasing torsion angle. On the other hand, the deformation curve for the oxidised implants, was characterised by a sharp increase at higher torque and a distinct breakpoint with shorter or no plateau period.

The gene expression in implant-adherent cells of the two implant types was analysed regarding 3 major processes: inflammation, bone formation and bone resorption. IL-1β was higher at the machined versus oxidised implants by factors of 3, 2.4 and 2.3 after 6, 14 and 28d of implantation, respectively. Similarly, the expression of TNF-α was higher at the machined implants by factors of 3 and 2.9 at the machined implants after 6d and 28d, respectively. Regarding the bone formation genes, a higher expression of OC was detected at the oxidised implants compared to the machined ones during all evaluation periods. The transcription factor, Runx2, showed 1.7-fold higher expression at the oxidised implants compared to machined at 28d time point. With respect to bone resorption genes, a higher expression of TRAP (at all evaluated time points) and CatK (at 6 and 14d) was demonstrated at the oxidised surface compared to the machined surface.

The BS-SEM showed that the threads contained mineralised lamellar bone and areas of newly formed bone with typical osteocyte lacunae and blood vessels. Direct contact between the oxidised implants and bone was observed with bone ingrowth into the micron- and sub-micron pores.

Surface characterisation revealed that the oxidised implant surface had higher roughness parameters (moderately rough) compared to the machined surface. Furthermore, the chemical analysis revealed 3.6% phosphorus in the oxidised surface. The surface oxide thickness reached up to 7.5 μm as judged by the in-depth profiling. TEM showed that the surface oxide consisted of both amorphous as well as crystalline phases. The crystalline phase was identified to be anatase.

Paper III

In study III, the kinetic changes in structure and composition of bone interfaces was investigated and related to the expression of bone remodelling genes, over an extended period of time (1d-28d).

The histological/histomorphometric analysis demonstrated higher percentage of bone in contact with oxidised implant (60% BIC) compared to machined implants (40% BIC), both at 14 and 28d. The bone area percentage (BA), occupying the threads, was higher at the oxidised implant after 6d, whereas at the later time points (14d and 28d) the machined implants was associated with higher BA percentage compared to the oxidised implants.

The BS-SEM revealed a progressive maturation of bone over time with a predominance of immature, less mineralised bone in the implant threads at 6d and well-mineralised, highly remodelled, bone after 28d. Bone tissue could be seen growing into the porous surface of the oxidised implant. This was further confirmed in the ultra-structural TEM analysis where bone ingrowth was observed even in the sub-micron pores. Collagen fibres were found in parallel direction to the surface. The EDS chemical analysis revealed the presence of calcium and phosphorus inside the sub-micron pores of the oxidised implants.

Gene expression analysis at 3d revealed a 65-fold higher expression of OPG at oxidised implants compared to the machined implants. Furthermore, 41- and 77-fold higher expression of RANK and RANKL, respectively, were demonstrated for oxidised implant compared to machined at 3d. The RANKL/OPG ratio was higher at the oxidised implants compared to machined implant after 1d of implantation. This difference was reversed after 3d, where a higher RANKL/OPG gene expression ratio was found at the machined implants. Thereafter (6d and 14d), a higher RANKL/OPG ratio was found again at the oxidised implant. No difference was observed at 28d. For both implant types, the RANKL/OPG ratio increased from 1d to 14d and was significantly reduced after 28d.

Correlation analysis between the analysed genes of bone remodelling at 3d revealed strong, positive relationships between RANK, RANKL and OPG only at the oxidised implants, but not the machined.

Paper IV

In study IV, an *in-vitro* model was developed with the aim to determine cell-specific adhesion and gene expression of monocytes and MSCs in mono- and in co-cultures, when adhering to titanium implants, and to study the protein profiles of the implant-adherent monocytes and MSCs in mono- and co-cultures.

The cell counting and FACS analyses revealed that after 24h, *in vitro*, the coexistence of monocytes and MSCs in co-culture led to equal proportions of adherent monocytes and MSCs, irrespective to implant type. In contrast, a higher proportion of adherent monocytes was found when cells were in mono-culture on the oxidised implant.

SEM revealed that the monocytes and MSCs in the co-culture were in close proximity and at times with direct connection between the cellular processes suggesting a direct cell-cell interaction.

The qPCR analysis of FACS-sorted cells revealed that the coexisting surface-adherent monocytes and MSCs, in co-culture, up-regulated the expression of IL-1β, in monocytes, and IL-1β and CXCR4, in MSCs, compared to that detected in mono-culture. In addition, in co-culture, the expression of BMP-2, SDF-1 and integrin-β1 was mainly enhanced in the implant-adherent MSCs, but not in the monocytes. No major differences between the two implant types could be observed in the present, un-stimulated, culture conditions.

ELISA showed that BMP-2 was not secreted by surface-adherent monocytes in mono-culture, but significantly enhanced when monocytes were present with MSCs in co-culture.

As judged by the protein profiling, several cytokines, chemokines and growth factors were enhanced when monocytes and MSCs co-existed on the implant surface, and these included: MCP-1, IL-6, CXCL5, VEGF-A and CSF-1. Furthermore, several factors were mainly secreted by the MSCs in the mono-culture, and their secretion was enhanced in the co-culture, which included: MMP-1, MMP-10, LIF and OPG. In contrast, MIP-1α and CASP-8 were highly secreted by the monocytes in the mono-cultures, however, their secretion did not change in the co-culture. The only factor showing a reduction in the co-culture was the CXCL10, which was mainly secreted by the monocytes in mono-culture.

Paper V

In study V, thirty patients, with transfemoral amputation (TFA), using osseointegrated, percutaneous titanium implants, and who had been scheduled for abutment exchange were consecutively enrolled. The aims were to determine the macroscopic skin signs, the presence of bacteria and the gene expression in abutment-adherent cells and to conduct correlative and comparative analyses between the different parameters.

Redness and a granulation ring were present in 47% of the patients. The modified Holgers skin score of 2 was the most frequent.

The most frequent radiological changes of the bone around the fixture were proximal trabecular buttressing (14/30 patients) and endosteal bone resorption (10/30). Pain upon loading was experienced by 8/30 patients whereas 3/30 patients declared pain at rest.

Bacteria were detected in 27/30 patients, most commonly in the bone canal. The most common bacteria were *Staphylococcus aureus*, coagulase-negative staphylococci, streptococci and *Enterococcus faecalis*.

A positive correlation was found between the expression of TNF-α in abutment-adherent cells and the detection of *S. aureus* irrespective of sampling site. *S. aureus* together with other bacterial species revealed a positive relationship with MMP-8 gene expression. A negative correlation was demonstrated between the residual length of the stump and the detection of a granulation ring around the abutment, and the detection of *E. faecalis*. No correlation was found between fixture loosening and bacteria in the skin-penetrating site (SPS). In addition, no correlation was detected between endosteal bone resorption and bacteria in the SPS, on the abutment and in the bone canal. A positive correlation was found between fixture loosening and two other clinical parameters: pain symptoms, and radiological detection of endosteal bone resorption. Fixture loosening was also correlated with a reduced expression of anti-inflammatory interleukin-10 and osteogenic differentiation marker osteocalcin in abutment-adherent cells.

5 DISCUSSION

In the present thesis, a methodological platform was developed in order to advance our scientific understanding of the mechanisms of osseointegration. Special emphasis was placed on the cellular activity in the implant-tissue interface, particularly during the initial stages of osseointegration. Paper I focuses on the initial events of inflammation, cell recruitment and adhesion. The inflammatory, osteogenic and osteoclastic responses were the focal point in Paper II. Here, we combined the molecular findings with an evaluation of functional effects (biomechanical evaluation). In Paper III, the relationship between molecular and morphological patterns at the interface was studied, with particular reference to bone remodelling. Efforts to explore the response of specific cell types were pursued in an *in-vitro* mono- and co-culture model (Paper IV). In the final work (Paper V), qPCR methodology was employed for the analysis of implant-adherent cells on retrieved skin-penetrating abutments, connected to osseointegrated amputation prostheses. The results were correlated to microbiological and clinical findings.

5.1 Initial events of cell recruitment and adhesion in the bone-implant interface

Immediately after the insertion of an implant, a sequence of cellular events is initiated. One of the hallmarks is the recruitment of cells to the site of injury, including the implant surface and the surrounding tissue[43]. In Paper I, both inflammatory cells and mesenchymal osteoprogenitors were detected at an early stage both in the tissue and in the proteinaceous matrix adhering to the implant. In the search for a tentative molecular explanation for the recruitment of different cell types, the expression of selected cytokines and chemokines in implant-adherent cells was explored. According to the prevailing concept of inflammation, bone regeneration and remodelling in the implant-bone interface, the recruitment of MSCs, bone regeneration and remodelling appear quite late (3-10 days and 4 weeks respectively)[88]. In contrast, the present findings provide evidence that the recruitment of MSCs and osteoprogenitors takes place much earlier and, in fact, simultaneously with the inflammatory cells during the initial hours after implantation. One of the main observations during the initial 24h was the modulation of the chemokine receptor, CXCR4, in implant-adherent cells (Paper I). CXCR4 is the receptor for the chemokine, SDF-1, which is a major mediator of MSC recruitment to the site of injury. The CXCR4/SDF-1 is a major axis for MSCs migration *in vivo*[125] and it is regarded as the axis of choice for enhancing

chemokine-mediated MSC homing to the site of injury in tissue engineering[42]. It has also been suggested that the CXCR4/SDF-1 pathway plays a crucial role in bone formation, where it is involved in the migration of circulating osteoblast progenitors to the site of bone regeneration in BMP-2-containing collagen pellets in mouse muscles[126]. Interestingly, the present findings show that implant surface modification strongly enhances the expression of CXCR4 in the implant-adherent cells. This was demonstrated by the observation that oxidised implants promote 11-fold higher expression of CXCR4 compared with the machined ones after 12h of implantation. Whereas, in the *in-vivo* study (Paper I), the exact phenotypes of the implant-adherent cells that expressed the CXCR4 were not determined, immunohistochemistry revealed that a large population of cells in the peri-implant tissue were positive for periostin, a marker of osteoprogenitors. Furthermore, SEM analysis showed that a high proportion of large, mesenchymal-like cells adhered to the oxidised implants. In an attempt to address the cell types responsible for the expression of CXCR4 and SDF-1, the results in Paper IV revealed two main related findings: firstly, the results showed that, in a co-culture of monocytes and MSCs adhering to machined and oxidised implants, only the MSCs expressed SDF-1. Secondly, although the MSCs *per se* did not express CXCR4 in a mono-culture, they significantly upregulated the CXCR4 expression when co-existing with monocytes.

In parallel with the upregulation of chemotactic signals for MSCs, the results of the *in-vivo* study (Paper I) showed that the expression of chemokines crucial for the recruitment of inflammatory cells, including PMNs and monocytes, was modulated during the first 24h after implantation. Furthermore, the results in Paper I showed that the expression of the selected chemokines in the implant-adherent cells was largely influenced by the different surface properties of machined and oxidised implants. Both surfaces were associated with the significant temporal upregulation of IL-8R and MCP-1 gene expression between three and 12 hours after implantation. IL-8R is a marker of PMN recruitment and MCP-1 is a major chemoattractant protein for monocytes/macrophages[35]. Whereas the expression of IL-8R was transiently upregulated after 12h, for both surfaces, MCP-1 expression continuously increased at machined but not oxidised surfaces. The finding for IL-8R gene expression is in line with the short life span of PMNs at the sites of inflammation and did not appear to be affected by implant surface modification, as no differences were found between the two implant surfaces. These results are supported by a previous *in-vitro* study, where leukocyte adhesion (mainly PMNs) to machined and oxidised surfaces increased during the first hours of blood-material contact and decreased thereafter[120]. On the

other hand, the expression of MCP-1 revealed a constant increase to the highest level after 24h, particularly at the machined implants. This was in parallel with a higher expression of both TNF-α (after 3h) and IL1β (after 24h) in the cells adhering to machined surfaces compared to oxidised surfaces.

The change in gene expression between the surfaces during these early time points can be due to several possible mechanisms. As blood clot formation is the start of the healing process, the interaction between blood and material is regarded as one important factor for successful implantation[127-129]. Cells that come into contact with surfaces adsorbed with proteins do not directly "sense" the substrate but instead interact with the intervening protein adsorbate[130]. In the present thesis, no detailed characterisation was made of proteins adhering to the different surfaces. However, in Paper I, a general observation in all histological sections (and supported by SEM) was the large amount of fibrin-like tissue with entrapped leukocytes and erythrocytes covering the machined surface. Fibrinogen has been shown to enhance the pro-inflammatory response to biomaterials[131] and may tentatively be involved in the upregulated gene expression of inflammatory markers at the machined surface. In addition, albeit not explored in this thesis, another protein cascade that can be differently activated by the two implant types is the complement pathway. In contrast to materials inserted in the blood vasculature[72], little is known about the involvement of the complement system in association with materials in bone. A previous study showed that metals with different surface properties induced very different thrombogenic and complement activating patterns[71].

In addition to the possibility that the implant surface topography and chemistry influenced the protein-mediated effects on the implant-adherent cells, the differences in material surface topography and chemistry may also have affected the shape and orientation of the cells. The surface topography may play a role in the orientation of a cell and ultimately guide the direction of migration. For instance, cells on a grooved surface become oriented with the grooves and migrate in the direction of the grooves, not across them[132]. Furthermore, there is evidence *in vitro* that the cell shape may regulate gene expression[133].

The attachment of the cell to a surface is one of the first critical steps in the cellular response to a biomaterial[88]. In the *in-vivo* experiments, the number and proportion of different cells adhering to the implant surface was not determined. One way of assessing the proportion of cells, as well as quantifying the specific cell types in the overall population of implant-

adherent cells, is flow cytometry or FACS[122]. This was performed in the *in-vitro* study (Paper IV) using screw-shaped implants similar to those used in Papers I-III. When monocytes and MSCs were cultured alone, monocytes preferentially adhered to the oxidised surface compared with MSCs. A similar observation was made with the polystyrene (Ps; control surface) but not the machined surface. One possible explanation of this observation is the increased texture and rugophilia provided by the oxidised surface. Previous observations *in vitro* have described this important concept[134,135]. On the other hand, the Ps surface also displayed a similar response, despite being smooth. Here, the surface chemistry may play an important role. Admittedly, the *in-vitro* system needs to be further characterised with respect to material surface-adsorbed proteins and the available material surface area for the adhesion of cells. One important observation was the different distribution of adherent cells (compared with mono-cultures) when they were in co-culture. Here, the two titanium surfaces revealed 60% MSCs and 40% monocytes, whereas the Ps demonstrated a monocyte predominance. This suggests that the surface properties, as well as the cell-cell interactions, play a role in determining the relative proportions of these two cell types when settling on the implant surfaces.

Integrins mediate interactions between cells and between cells and extracellular matrix[43]. In the present *in-vivo* model, integrin-β1 and -β2 showed a peak at 12h for both machined and oxidised implants. Further, the expression of integrins-β2 (after 12h) and -β1 (after 24h) was significantly increased at oxidised implants compared with machined ones. Whereas integrin-β1 is expressed by different cell types, including inflammatory cells and MSCs, integrin-β2 is exclusively expressed by leukocytes. Interestingly, the co-culture of monocytes and MSCs *in vitro* (Paper IV), on the machined and oxidised implants, revealed that the integrin-β1 is predominantly expressed by MSCs. Taken together, the present results show, firstly, that integrins are rapidly expressed in the implant-adherent cells *in vivo* and, secondly, that implant surface modifications may enhance integrin expression, possibly in a cell-specific manner. The finding that modified surfaces enhance the expression of integrin-β1 is in line with previous *in-vivo*[136] and *in-vitro* studies[137]. On the other hand, the expression of integrin-β2, which is exclusively linked to leukocytes, at the oxidised implants did not appear to be associated with increased inflammatory activity. One explanation is that the increase in β2 expression at the oxidised surface might be related to osteoclast progenitors[138].

Integrins and chemokines are triggered and expressed simultaneously during the early phase of cell recruitment. In the present *in-vivo* model, positive

correlations were demonstrated between the expression of chemokines and integrins in implant-adherent cells after 24h[139]. In particular, IL-8R was associated with integrin-β2, whereas MCP-1 showed a relationship with integrin-β1 and -β2. Interestingly, at the oxidised surface, CXCR4 was positively correlated with integrin-β1, which provides supporting evidence for a predominance of MSCs on the oxidised surface *in vivo*. The machined surface, on the other hand, demonstrated a strong correlation between CXCR4, IL8R and integrin-β2, which points in the direction of more leukocytes being associated with this surface.

5.2 Monocyte-MSC interactions

In Papers I-III, the analyses were performed on all implant-adherent cells. In Paper IV, the cell-specific gene expression was analysed in monocytes and MSCs separately and in co-culture. There were no major differences between the two titanium surfaces, irrespective of mono- or co-cultures and cell type, either at gene expression level or for protein secretion. One possible explanation of the discrepancy between the *in-vitro* findings and the previous gene expression data *in vivo* is the different environmental conditions, e.g. that no inflammatory stimuli were added in the *in-vitro* model, which would partly have mimicked the early inflammatory response *in vivo*. Interestingly, the sorted MSCs, when co-cultured on implant surfaces, had higher IL-1β gene expression compared with mono-culture conditions. This finding suggests, firstly, that monocytes mediate signals for the enhanced IL-1β expression by MSCs and, secondly, that the MSCs may acquire pro-inflammatory potential. The former novel finding may be of importance for the transition between the inflammatory and regenerative phases *in vivo*. The latter suggestion is in line with previous *in-vitro* findings that MSCs can be primed to either pro-inflammatory or immunosuppressive phenotypes, depending on specific signals in the surrounding environment[140]. The mechanism responsible for the augmented response remains to be established.

Several interactions between monocytes and MSCs were indicated when comparing the secretory profiles of the cells when cultured alone or together. One important finding was that the co-culture of monocytes and MSCs in direct contact resulted in a significantly higher level of leukemia inhibitory factor (LIF) compared with that produced by MSCs alone. LIF is a factor that is implicated in the immunosuppressive effects of MSCs on leukocytes and inflammatory cells[141,142]. Furthermore, LIF acts on bone stromal cells to enhance differentiation into bone-forming osteoblasts[142] and has an inhibitory

effect on the expression of sclerostin, a potent inhibitor of bone formation[143]. The enhanced LIF secretion in the co-culture indicates that the cross-talk between the two cell types also involves regenerative and/or immune-regulatory signals. This is supported by the ELISA findings showing that the release of pro-osteogenic factor BMP-2 from MSCs is enhanced when the MSCs co-existed with monocytes in co-culture. Like LIF, other analysed growth factors (VEGF-A, CSF-1 and OPG) were highly secreted in the co-cultures, which further supported this assumption. Moreover, and contrary to all other profiled cytokines, CXCL10 revealed a lower level in the co-culture compared with the mono-culture of monocytes. Increased CXCL10 mRNA and protein expression has been associated with the pathogenesis of various infectious diseases, chronic inflammatory diseases and immune dysfunction[38]. CXCL10 has also been shown to correlate with the rejection of certain organs after transplantation[144]. The present finding of reduced CXCL10 in the co-culture of MSCs and monocytes provides additional support for the assumption of an immunosuppressive role for the MSCs.

5.3 Inflammation at the bone-implant interface

Following the initial blood/material interactions and the formation of a provisional matrix, a sequence of acute and chronic inflammation occurs[145]. The inflammatory response around the inserted implant has several important roles in the healing process, such as removing debris from the surgical trauma and sending the appropriate signals to start the repair and regeneration process. In Paper I, during the initial 24h, the machined surface was associated with higher inflammatory activity, indicated by the higher gene expression of TNF-α and IL1β. In the later period (after the early stage of woven bone formation), up to 28d (Paper II), the expression of the pro-inflammatory cytokines for both implant surfaces was relatively constant, although still significantly higher for the machined surfaces. These observations suggest that the physico-chemical properties of the implant surface play a major role in triggering and modulating inflammation. The temporal modulation of TNF-α might be important for the bone-remodelling phase, as indicated in a previous *in-vivo* study, where the peak expression of TNF-α coincided with the highest gene expression for OC, ALP, TRAP and CatK three days after implantation[139]. This assumption was further confirmed by significant correlations between TNF-α and Runx2, ALP, TRAP, CatK for the oxidised surface alone (Paper II).

The early inflammatory response to implanted biomaterials has been described as an essential process that determines wound healing and implant

integration or failure[3,146,147]. In spite of this, the impact of pro-inflammatory cytokines *in vivo* is highly controversial. High yet transient levels of pro-inflammatory cytokines, e.g. IL-1β, IL-6 and TNF-α, have been observed around implants during the early hours after implantation *in vivo*[148]. However, a prolonged association with pro-inflammatory cytokines around implants can be detrimental, as activated inflammatory cells can induce osteolysis and ultimately aseptic loosening[147,148]. During bone defect healing with and without bone substitutes, several positive correlations were found between the expression of TNF-α and the expression of bone formation (ALP) and bone remodelling (TRAP and CatK) genes and this was mainly detected in the defects treated with synthetic substitutes[149]. In the latter study, however, the level of TNF-α did not differ between the sham, untreated and the defects treated with the synthetic substitute. The present study (Paper II) shows a positive correlation for TNF-α with osteogenic and bone-remodelling genes at the oxidised implants, where the overall TNF-α expression was significantly lower compared with the machined ones. Taken together, the results indicate a plausible osteogenic- and osteoclastic-promoting effect of TNF-α in conjunction with bone formation and remodelling at biomaterials, which is probably dependent on the level of expression of this cytokine.

5.4 Bone regeneration and remodelling at the bone-implant interface

The oxidised implants demonstrated higher gene expression for bone formation and remodelling markers at both the early and later time points (Paper II). In fact, the peak expression of OC, ALP, TRAP and CatK has been observed as early as three days after implantation[139]. On the basis of the results in Paper III, it was shown that cells adhering to oxidised implants promote not only early osteogenesis and bone formation but also osteoclastogenesis and remodelling activity, via the RANKL/RANK/OPG triad. Osteoclasts differentiate and become activated when RANKL on the osteoblasts binds to RANK on osteoclasts. Three days after implantation, only the oxidised surfaces triggered high expression levels of RANKL and RANK in the implant-adherent cells. In the same way, OPG, the break for RANKL, was only upregulated at the oxidised surface. The early enhanced osteoclastic differentiation coupled to osteoblast differentiation at the oxidised surface is supported by the positive correlation between RANK and RANKL expression, which was not observed for the machined surface. The ratio between RANKL and OPG has commonly been used to index the level of bone remodelling. For both machined and oxidised implants, the highest

RANKL/OPG ratio was observed between three and 14 days, corresponding to the bone-remodelling phase in this model. The finding that a larger amount of mineralised bone was in contact with the oxidised surface suggested accelerated bone maturation, pushed by an increase in the RANKL/OPG ratio at this surface.

One important question is which cells express and secrete these regulatory molecules *in vivo*. According to the literature, in the bone environment, stromal cells, osteoprogenitors and osteoblasts express both RANKL and OPG, whereas RANK is mainly expressed by osteoclast progenitors and osteoclasts[18,150]. Other cells, such as fibroblasts, dendritic cells and T-lymphocytes, are also able to express RANKL and OPG[18]. In Paper IV, the protein levels of OPG were analysed for monocytes and MSCs in mono-culture as well as in co-culture. Firstly, the data indicate that MSCs are responsible for the OPG secretion obtained in the co-culture. Secondly, no differences were found between the machined and oxidised surfaces at protein level at the analysed time point. Although these findings underscore the importance of the *in-vitro* co-culture system, they also illustrate that the *in-vitro* and *in-vivo* models do not share the same features.

The exact reasons for the accelerated expression of bone formation and remodelling genes and the subsequent enhancing effects on bone formation, bone remodelling and osseointegration at the oxidised implants are still not clear. The main explanation of these two effects is a result of the combined effects of the physico-chemical surface characteristics, eliciting well-organised, highly regulated cellular and tissue responses.

Two main surface features of the oxidised implant, compared with the machined, are the increase in micron-scale roughness and the porous structure of the surface layer (Paper II). SEM images (Papers I and IV) showed mesenchymal cells with a firm attachment to the oxidised surface, extending cellular processes into the pores. The machined surface, on the other hand, was merely associated with fibrin-like tissue with numerous erythrocytes and leukocytes. Furthermore, the SEM revealed that the oxidised surface exhibits roughness features on the micron- and sub-micron scales. The important role played by micro-scale surface roughness in improved implant stability and bone formation is well documented[151]. On the other hand, less information on the role of nano-topography *per se* is available[3]. Our data on an increase in the expression of osteogenic markers in cells adhering to relatively rougher surfaces are in line with other *in-vivo*[87,152] and *in-vitro* observations[153,154]. On the nano-scale, recent studies revealed that nano-topography *per se* elicits less peri-implant macrophage infiltration and

significantly downregulates the expression of pro-inflammatory cytokine (TNF-α) in the cells adhering to nano-patterned titanium implants compared with machined implants[155]. As the present oxidised titanium implants have a combination of micro-scale and nano-scale topography, it is possible that the downregulatory effect on pro-inflammatory cytokine gene expression is predominantly related to nano-topography.

The AES and EDS analyses (Paper II) revealed a considerable and relatively constant amount of phosphorus throughout the oxide layer, reflecting a difference in chemical composition from that of the machined implants. The surface chemical composition may affect the hydrophilicity of the surface and highly hydrophilic surfaces appear to be preferred by cells, tissues and biological fluids compared with hydrophobic ones[156]. Anderson *et al.* suggested that the surface chemistry of a biomaterial dictates the degree of cellular cascade effects and ultimately determines the overall biocompatible outcome[43].

The ultrathin sections of the oxidised implant displayed a substantially thick oxide layer. This was confirmed by the depth profiling using AES and argon sputtering, revealing a thickness of 7.5 μm in the oxide layer for the oxidised implants. Further, this thick oxide layer demonstrated large clusters of crystalline structure (mainly anatase) embedded in amorphous titanium dioxide. Little is known about the effect of the phase composition of the surface oxide on the cellular and molecular events of osseointegration *in vivo*[3]. Early *in-vivo* studies showed that the anodic oxidation of electropolished titanium implants, producing a thick, rough surface oxide layer, enhanced the rate of bone formation[157]. Other *in-vivo* studies revealed an increase in removal torque after six weeks in rabbit tibia in parallel with the increase in oxide thickness of up to 3.4 μm[158]. However, in the latter study, the positive effect of the oxide thickness on osseointegration could not be isolated from the effect of other surface parameters, including different roughness, porosity and chemistry[158].

5.5 Implant stability and osseointegration

The combination of the *in-vivo* model with removal torque enabled the analysis of the relationship between cellular activity and biomechanical capacity at the interface. A significantly higher removal torque was demonstrated for oxidised implants at 14d and 28d. Furthermore, a significantly higher increase in removal torque over time was shown for the oxidised implants. One plausible explanation of the increase in implant stability at the oxidised implants (Paper II) is the increased amount of mature,

well-mineralised, and remodelled, bone in direct contact with the implant surface, as demonstrated for the oxidised implants (Paper III).

Although it is not clear which of the oxidised surface properties (roughness, porosity, chemistry and/or surface oxide thickness) plays the major role, the mechanisms for the increase in osseointegration at the oxidised surface involve enhanced and coupled bone formation and remodelling activities (ALP, OC, CatK and TRAP) which are fine-tuned by changes in the RANK/RANKL/OPG triad. One important finding is that these processes take place in cells adhering to the surface rather than those in the peri-implant bone. This fact can also provide an explanation of the ultrastructural observations, showing bone-like mineralised deposits inside the micron- and sub-micron pores of the implant surface layer. At the early time points, it was observed by SEM that MSC-like cells extend their cytoplasmic processes inside the pores of the oxide layer (Paper I), where deposition and/or mineralisation may take place. However, as the presence of collagen inside the pores could not be clearly seen by TEM, it is difficult to say whether the calcium- and phosphate-containing tissue found within the pores may be considered bone or not (Paper III). Nevertheless, it is likely that the direct coalescence of mineralised bone with the implant surface at ultrastructural level made a major contribution to the increased stability of the oxidised implant.

5.6 Clinical application

In Papers I-IV, sampling and analytical tools were developed and implemented in experimental animal and *in-vitro* models to enable detailed molecular analyses during the early stages of osseointegration of different titanium implants. In these papers, the analyses were performed on the implant-adherent cells, showing that these cells are the major contributors to the molecular activity at the bone-implant interface.

The treatment of individuals with transfemoral amputations using osseointegrated fixtures improves ambulatory function and the overall quality of life[159]. In Paper V, the sampling procedure was employed clinically on abutment-adherent cells of individuals with percutaneous titanium implants. In these patients, the abutment penetrates through the skin, thereby creating a breach in the skin barrier, which may be of importance for the host defence, bacterial colonisation and the maintenance of osseointegration. In a group of 30 consecutively enrolled patients with mechanical problems with their abutments, the gene expression was analysed and related to observations in the skin, the presence of bacteria and radiological changes around the

osseointegrated fixture. The macroscopically observed inflammatory signs in the skin (redness, secretion) and regenerative (granulation tissue) response were considerably more frequent compared with macroscopic inflammatory signs in the skin around percutaneous, bone-anchored hearing aids (BAHAs)[160]. Several possible factors, such as the major differences in anatomy and the mechanical forces imposed on the bone and soft tissue in the two regions, might explain this. Moreover, the previous trauma of lower extremity amputation may be important, as the skin of the stump is considered to be more fragile and prone to skin problems.

Bacterial colonisation was very frequent: 27 of 30 patients had positive cultures of potentially pathogenic species such as *Staphylococcus aureus,* CoNS, various groups of streptococci, *Enterococcus faecalis* and *Enterobacter*. Only three patients therefore displayed negative cultures at all sampling sites and about half the included patients had positive cultures for more than one bacterial species. However, only one patient had a clinical manifestation of infection in the skin-penetration site (SPS), septic loosening of the fixture and a definite diagnosis of deep infection (according to the definition in Tillander *et al*., 2010) at the time of observation. The most frequently found bacterium among these patients was *Staphylococcus aureus*, in agreement with Tillander and co-workers[97]. Importantly, we observed a high proportion of patients (20%) with a positive culture of *Enterococcus faecalis* in the bone canal. We also found a relationship between *E. faecalis* and a shorter stump. This finding could be important in relation to enforced and specific cleaning tools and instructions to patients, as well as the judgement of the residual extremity length before treatment. The high frequency of bacterial colonisation on the skin, on the abutment and in the bone canal indicates that the frequently observed macroscopic inflammatory signs are associated with a high bacterial burden. Support for this assumption is provided by the fact that the presence of bacteria in the skin (irrespective of species) and the presence of *E. faecalis* were associated with macroscopic signs of skin secretion and a granulation ring respectively.

The most commonly observed radiological changes in our study were proximal trabecular buttressing (increase in the density of the bone) and endosteal bone resorption (resorption of bone around the threads of the fixture). A variety of radiological changes in the fixture-bone interface have previously been described[161]. In our material, three patients had to remove their fixtures; their abutments were examined in exactly the same way as the remaining 27 abutments (in addition, this allowed sampling from the marrow cavity). Despite the small number of fixture removals (n=3) and the heterogeneous population, one important finding was the correlation between

fixture loosening and pain symptoms and endosteal bone resorption respectively.

In the current study, the method for sampling and RNA extraction was developed at our laboratory and the panel of genes representing tissue metabolism, bone physiology and cytokines was selected to give an overview of changes that might occur in the tissue/biomaterial interface of patients with osseointegrated implants.

IL-6 expression in abutment-adherent cells was positively correlated with the detection of polymicrobial cultures. IL-6 has been suggested as a biomarker for the diagnosis of infection[162]. Similarly, MMP-8 expression correlated with polymicrobial cultures, as well as with the detection of *S. aureus,* together with other bacterial species. MMP-8 is a collagen-cleaving enzyme involved in tissue remodelling[46]. These findings are in line with previous studies of inflammation around percutaneous, bone-anchored hearing aids, showing higher protein levels of IL-6, TNF-α and MMP-9 at inflamed sites[163].

Paper V also demonstrated a relatively higher gene expression of the pro-inflammatory marker, TNF-α, in association with positive cultures of *S. aureus* (irrespective of sampling site). The level of TNF-α in peri-implant crevicular fluid has previously been shown to be increased in patients with peri-implantitis compared with healthy subjects and the level was decreased after anti-infective therapies[164].

One important observation was the positive correlation between fixture loosening and a lower expression of IL-10. The roles of IL-10 in the maintenance or failure of osseointegration are not well understood. This is exemplified by contradictory observations in the dental literature on patients with peri-implantitis[30]. Furthermore, whereas a study suggested that IL-10 could provide information about the potency of the immune response in patients with peri-implantitis[165], another study reported no difference in IL-10 levels between patients with peri-implantitis and healthy subjects[164].

IL-10 is generally regarded as an anti-inflammatory cytokine which is implicated in the control of the inflammatory response[166] and a regulator of immunity to infection[167]. IL-10 also induces the expression of tissue inhibitors of metalloproteinases (TIMPs) and OPG, the respective inhibitors of MMPs and RANKL systems, thereby being implicated in the prevention of bone resorption[168]. In the present clinical study (Paper V), although a cause-effect relationship was not identified, the detection of *S. aureus* in high

frequency in the bone canal was associated with an increase in the expression of TNF-α and MMP-8, suggesting a mounted inflammatory response, presumably in order to clear the bacteria. On the other hand, no correlation was detected between the presence of bacteria and IL-10 expression. Albeit speculative, the multiple clinical signs of skin inflammation, an abundance of bacteria and an increase in pro-inflammatory gene expression present a risk scenario leading to the degradation of the bone holding the fixture. A prerequisite for a scenario of this kind to occur at the fixture-bone interface is that pro-inflammatory/degradation signals and inflammatory cells would reach and migrate respectively to the actual fixture-bone interface. A process like this would be balanced by anti-inflammatory activity and pro-regenerative activity. This hypothesis is supported at least in part by the finding that the three patients who had fixture loosening demonstrated a lower anti-inflammatory IL-10 and lower pro-osteogenic OC gene expression in abutment-adherent cells compared with the patients with fixture stability.

The data presented in Paper V underscore the necessity for future studies of the relationship between the bacterial species and the particular strain virulence, including biofilm properties and antibiotic susceptibility. The present approach to sampling and analysing the gene expression in cells present in the soft tissue-abutment interface is a first attempt to acquire a molecular understanding of the biological processes in this region. Finding an accurate combination of biomarkers could be essential in order to differentiate between pathogenic conditions (e.g. aseptic loosening and low-grade infection) and the establishment of prevention protocols.

5.7 Methodological considerations

The sensitivity, reproducibility and specificity of a method set the limits for the quality and reliability of the experimental data. For this reason, a critical assessment of the scientific methods is a key feature of research. In the present thesis, *in-vitro, in-vivo* and human samples were analysed. Interest has focused on the development of a methodological platform to study the cellular and molecular events in combination with a structural and functional evaluation of the biomaterial-tissue interface.

5.7.1 Sampling

One major point of emphasis in this thesis was the sampling and methodological development. One advantage of the present *in-vivo* model was the opportunity to isolate the RNA from both implant-adherent cells and the peri-implant bone. This allowed for the spatial distinction of gene

expression between the cells in contact with the implants and in the tissue some distance from the implant. Differences between the two implant surfaces were frequently detected in the implant-adherent cells rather than in the peri-implant bone. However, the implant-adherent cells constitute a small amount of biological material, which requires highly optimised RNA-extraction procedures. This resulted in limitations in quantifying the RNA and RNA quality control. On the other hand, this was successfully performed in the bone samples, which compensates for some of the information on the RNA quality that was lacking, as the samples were treated in similar ways. The normalisation in the first studies (I-III) was performed using 18S as a representative reference gene. In the human clinical study, a panel of human reference genes was employed and the mean of three stable reference genes was used. In the *in-vitro* studies, the normalisation was made with the number of FACS-sorted cells.

The analysis of the abutment-adherent cells, in the clinical study (Paper V), reflects the cellular processes occurring in the soft tissue-abutment interface in the bone canal. The limited bone tissue in this area might be one reason for the lack of gene expression of the bone remodelling-related factor calcitonin receptor. In contrast to the experimental implants, the large size of the abutment did not allow for the traditionally used homogenisation methods. The lysis was therefore performed with upscaled volumes of reagents and rough vortexing. To confirm the complete detachment of cellular material, SEM was performed on randomly selected abutments after RNA/protein extraction. In addition, metallic ions and blood from the abutment could constitute potential inhibitors for the qPCR and, for this reason, inhibitory tests were performed and excluded these confounding factors.

The *in-vitro* sampling (Paper IV) was conducted on cells in mono-culture and co-culture. Trypsin was used for the detachment of both cell types and the incubation time was shortened as much as possible to avoid destroying epitopes. The detachment of cells was confirmed using SEM.

5.7.2 Molecular techniques

The core molecular technique used in the thesis is the qPCR. All primers were designed and validated to ensure efficiency and specificity. For immunohistochemistry (paraffin-embedded samples), the sample reflects the bone-implant interface and cannot be fully compared with the implant-adherent cells. In spite of this, one major advantage is the opportunity to identify different cell types, as well as the secreted proteins. One limitation of the paraffin-embedded samples is that they do not contain the actual implant.

For histomorphometry, bone-implant contact and bone area in the threads were determined in plastic-embedded ground sections that contain the implant.

The WB analysis of Protein A (Paper V) detects the protein in the cell wall of *S. aureus*. The RNA/protein-extraction method was optimised for eukaryotic cells, but the rough vortexing and extraction buffer are likely to lyse the bacterial cells, despite the thick cell wall of *S. aureus*[169]. The antibodies used in the current WB may also detect fragments of the bacterial cells, as well as dead bacteria that could not be detected on the culture plates.

5.7.3 Study design

Pre-clinical *in-vivo* models involving small animals are necessary platforms for basic research. No single *in-vivo* model exists that completely recreates the anatomical, physiological, biomechanical and functional environment of humans. The selected animal model should therefore reflect the question for which an answer is sought[170]. The rat tibia model used in Papers I-III has several advantages: it is very well studied, which makes it easy to relate these findings to previous studies. It is reproducible and many cellular events are well preserved between species (e.g. RANK/RANKL/OPG axis). The model makes it possible to analyse the gene expression of the implant-adherent cells, as well as the bone collar surrounding the implant.

At present, the need to further characterise the different cell types on the implant surface, as well as protein profiling, is challenging, due to the small number of biological samples and the poor availability of a panel of antibodies for the rat. We therefore chose the human *in-vitro* system to address these questions. Two major advantages of *in-vitro* studies are the reduced number of variables that affect the outcome and the opportunity to focus on specific cellular events during interactions either with a material surface or between particular cell types. The *in-vitro* co-culture models required a suitable culture medium that supports the balanced growth of both monocytes and MSCs. Based on a previous study[171] *in* which DMEM was successfully used for human monocytes and MSCs, this was also the choice in the current study. Another advantage of this *in-vitro* platform was the use of actual screw-shaped implants instead of titanium discs. The shape of the implant may influence the behaviour and activation of the cells and in this way we approached the clinical situation[172]. One disadvantage of this *in-vitro* platform is the need to pool the implants to reach a critical number of cells for counting.

In the clinical study (Paper V), patients scheduled for the exchange of the abutment were enrolled. This represents a potential selection bias, as the study could not be conducted on a randomly selected pool of transfemoral amputees. The abutment, which would otherwise have been discarded, provided valuable information using gene expression analysis and the sampling involved minimal interference with the clinical procedure. The anatomic conditions in the clinical study are unique and it is difficult to extrapolate these data to other applications, even to other percutaneous ones. In spite of this, the results might be useful for bone-anchored hearing aids where similar problems have been observed (skin inflammation, presence of bacteria and infection)[163].

6 SUMMARY AND CONCLUSION

The present thesis was performed *in vitro*, in animal studies and in humans.

- In Paper I, it was demonstrated that implant surface properties influence extracellular matrix protein and cell morphology, cell recruitment and gene expression at the bone-implant surface during the early time points after implantation. A higher gene expression of major MSC recruitment and adhesion factors (CXCR4 and integrin-β1) was revealed in cells adhering to oxidised implants compared with machined ones. This was corroborated by the predominance of MSCs at the oxidised surface, as judged by the immunohistochemistry and SEM morphological analyses. On the other hand, cells adhering to machined implants were associated with greater pro-inflammatory activity.

- In Paper II, the *in-vivo* model was combined with torque analysis, which enabled detailed studies of the complex interplay between material surface properties, cell activity and functional aspects. Oxidised implants demonstrated an increase in bone anchorage in association with the downregulation of pro-inflammatory genes (TNF-α and IL-1β) and the upregulation of bone-remodelling genes (ALP, OC, TRAP and CatK). The increase in biomechanical stability shown for the oxidised implants strongly suggests greater bone interlocking compared with machined implants.

- The results in Paper III showed that the oxidised implants rapidly stimulate bone formation and remodelling involving the regulation of the expression of the RANK, RANKL, OPG triad. These molecular determinants promote the process of osseointegration, characterised by a large amount of mineralised bone in contact with the implant surface and ultrastructural features suggesting a bonding between the mineralised tissue and pores in the oxide.

- In Paper IV, the results showed that, in an unstimulated and static culture condition *in vitro*, the co-existing monocytes and MSCs on the implant surface upregulate the gene expression of IL-1β and CXCR4 in a cell-specific manner compared with that detected when each cell existed alone on the implant surface. Furthermore, the gene expression of BMP-2, SDF-1 and integrin-β1 is mainly enhanced in the surface-adherent MSCs but not in the monocytes. As judged by protein profiling, the overall secretory profile of the surface-adherent monocytes and MSCs is synergistically enhanced when the two cell types co-exist on the implant surface.

- Finally, the results in Paper V showed that the macroscopically observed inflammatory signs in the skin (redness, secretion) and a granulation ring were observed in about 50% of 30 consecutively enrolled patients with a transfemoral amputation treated with osseointegrated fixtures and a percutaneous abutment. Bacterial colonisation was frequently detected on the skin, the abutment and in the bone canal. A higher expression of TNF-α was associated with positive cultures of *S. aureus*. Furthermore, positive associations were found between fixture loosening and the lower gene expression of IL-10 and OC in three patients with fixture loosening.

In conclusion, the present combination of comparative and correlative analytical techniques allows for detailed analysis of the cellular, molecular, structural, ultrastructural and biomechanical events at the bone-implant interface. Employing this methodological platform, it was demonstrated that implant surface properties elicit a cellular and molecular cascade for rapid cell recruitment and enhanced bone formation and remodelling which, in turn, accelerates bone maturation and the implant stability at the bone-implant interface. The present set of analyses suggests candidate factors, such as the RANKL/OPG expression ratio, as a sensitive indicator for monitoring the remodelling process during osseointegration. Finally, the results of the present thesis provide a first line of information on factors that could affect the performance of percutaneous implants.

7 FUTURE PERSPECTIVES

The findings from the clinical study indicated several relationships between clinical and microbiological assessments and the selected panel of qPCR markers. A future large-scale molecular array (on the RNA and protein levels) may provide information on other factors of importance in relation to tissue-integration, performance and/or the pathological changes in conjunction with osseointegrated implant-based procedures. Furthermore, it is of interest to gather more information on the bacteria related to biomaterial associated infections, for instance by employing the technique Next Generation Sequencing (NGS), in order to identify virulence factors and specific types of bacteria involved.

Based on the detailed studies on the mechanisms of osseointegration, several factors appeared to be crucial for the different processes. One example was the strong association between the molecular cascade involved in bone formation and remodelling and the higher degree of integration and stability of the implants. Future work may extend these findings into a clinical situation, e.g. monitoring RANKL/OPG gene expression ratio around bone-anchored implants in relation to the development of osseointegration.

The application of FACS in the *in vitro* model provided useful data on the cell-specific activities (e.g. adhesion and gene expression) when two known cell types were simultaneously present at titanium implants. The next step is to employ the FACS technique *in vivo* in order to characterise a more complex population of implant-adherent cells.

The *in-vitro* platform provided a sensitive system, which would allow inclusion of other cell types and to extend the analysis over different periods of time. Addition of stimuli, e.g LPS, would activate a series of intracellular signals leading to a rapid increase in pro-inflammatory cytokines. This would, at least partly, mimic the inflammation induced by trauma or infection following the insertion of an implant *in vivo*. Furthermore, the model provides possibilities to study other routes for cell-cell communication, for instance via exosomes. In addition, several factors appeared to be regulated differentially in the co-culture (e.g. LIF and CXCL10). These factors have not been studied in relation to tissue healing around biomaterials and deserve further exploration.

ACKNOWLEDGEMENTS

This work was supported by the BIOMATCELL VINN Excellence Center of Biomaterials and Cell Therapy, the Västra Götaland Region, the Swedish Research Council (K2012-52X-09495-25-3 & K2015-52X-09495-28-4), the LUA/ALF Research Grant "Optimization of osseointegration for treatment of transfemoral amputees" (ALFGBG-448851), the IngaBritt and Arne Lundberg Foundation, the Hjalmar Svensson Foundation, the Vilhelm and Martina Lundgren Vetenskapsfond, and the Area of Advance Materials of Chalmers and GU Biomaterials. The implants used in the studies (I-IV) were kindly provided by Nobel Biocare AB.

This thesis could not have been realised without the profound support I have received from my supervisors, colleagues and family. I am sincerely grateful to be surrounded by such great people and would like to express my thanks to:

First and foremost, my main supervisor, Peter Thomsen for giving me this opportunity and always giving me inspiration and encouragement. I am sincerely grateful for all your efforts especially during the finalising stage of these research projects.

Omar Omar, my co-supervisor, for your tremendous work and efforts in helping me reach the point where I am today. I will always be grateful for your commitment, friendship and for teaching me so much.

Mikael Kubista and Jukka Lausmaa, my co-supervisors, for scientific input and support throughout these years.

To all my co-authors, for your invaluable expertise and skilful work on our scientific papers.

Anna Johansson, Lena Emanuelsson, Maria Hoffman and Birgitta Norlindh for always helping out and for being caring and supportive through tough and happy times in life.

All my former and present colleagues at the Department of Biomaterials, especially: Anders Palmquist for your endless patience with my never ending IT-problems, Sara Svensson for great collaboration and your kindness, Margarita Trobos for generously sharing your bacteria-knowledge, Karin Ekström for your excellent skills and efforts during my years of FACS-

problems, Forugh Vazirisani for your commitment and encouragement, Furqan Ali Shah for proof reading and the brilliant cover photo, Carina Cardemil for your friendship and laughs, Annika Juhlin for being a great roomie and the daily discussions about life and research, Patrik Stenlund, Magdalena Zaborowska, Xiaoqin Wang, Ibrahim Elgali, Alberto Turri, Dimitrios Karazisis, Shariel Sayardoust, Felicia Suska, Nikos Papadimitriou, Louise Rydén, Behnosh Malekzadheh, Maria Utterhall, Magnus Wassenius, Petra Gunnarsson, Christer Dahlin, Pentti Tengvall and Tomas Albrektsson for support, laughs and fruitful discussions during coffee breaks.

All my clinical collaboration partners Georgios Tsikandylakis, Örjan Berlin and Rickard Brånemark for your expertise, time and efforts.

A special thanks to all my former and previous colleagues at TATAA for creating an inspiring work environment. In particular: Kristina Lind for sharing your great insight in method development, Jens Björkman for always setting aside time to help me move forward in my work, Robert Sjöback for your invaluable knowledge and guidance, Emelie Lott, Caroline Olsson, Petra Wallentin, Anne Hansen, Jennie Bengtsson, Cao Hui, David Svec and Hanna Mann for all your assistance.

Jan Hall for your kind support as external mentor, the nice lunches and for all your help in introducing me to materials science.

Siv Lindbratt Börjes for your invaluable mentorship that has evolved into our great friendship.

TACK alla mina fantastiska vänner för all glädje och energi ni ger mig! Tack Parshin för dina glada tillrop och hjälp med festfixeri!

Slutligen, tack min älskade familj för allt stöd och framförallt för att ni tagit så väl hand om min lilla ögonsten Mollie under de senaste månaderna av långa arbetspass. Tack Mamma för din enorma energi och generositet, Pappa för din imponerande drivkraft och förmedlan om att allt är möjligt, Andy&Angie för er humor och för att ni alltid finns där, Stickan&Gun för alla avkopplande träffar i Luttra; Linda, Örjan, Hampus & Elvira för all glädje ni sprider. Mollie, min solstråle, varje dag med dig gör mig lycklig.

Det största av alla tack går till min älskade Marcus för ditt otroliga stöd, och den kärlek och trygghet du sprider. Du dök upp när jag behövde det som mest och har givit mig allt det jag önskar i livet ♥

REFERENCES

1. Branemark PI, Adell R, Breine U, Hansson BO, Lindstrom J, Ohlsson A. Intra-osseous anchorage of dental prostheses. I. Experimental studies. Scand J Plast Reconstr Surg 1969;3(2):81-100.
2. Branemark PI, Hansson BO, Adell R, Breine U, Lindstrom J, Hallen O, Ohman A. Osseointegrated implants in the treatment of the edentulous jaw. Experience from a 10-year period. Scand J Plast Reconstr Surg Suppl 1977;16:1-132.
3. Palmquist A, Omar OM, Esposito M, Lausmaa J, Thomsen P. Titanium oral implants: surface characteristics, interface biology and clinical outcome. J R Soc Interface 2010;7 Suppl 5:S515-27.
4. Karsenty G. The complexities of skeletal biology. Nature 423 2003:316-318.
5. Gerstenfeld LC, Cullinane DM, Barnes GL, Graves DT, Einhorn TA. Fracture healing as a post-natal developmental process: molecular, spatial, and temporal aspects of its regulation. J Cell Biochem 2003;88(5):873-84.
6. Suda T, Takahashi N, Udagawa N, Jimi E, Gillespie MT, Martin TJ. Modulation of osteoclast differentiation and function by the new members of the tumor necrosis factor receptor and ligand families. Endocr Rev 1999;20(3):345-57.
7. Nombela-Arrieta C, Ritz J, Silberstein LE. The elusive nature and function of mesenchymal stem cells. Nat Rev Mol Cell Biol 2011;12(2):126-31.
8. Dimitriou R, Tsiridis E, Giannoudis PV. Current concepts of molecular aspects of bone healing. Injury 2005;36(12):1392-404.
9. Stein GS, Lian JB, van Wijnen AJ, Stein JL, Montecino M, Javed A, Zaidi SK, Young DW, Choi JY, Pockwinse SM. Runx2 control of organization, assembly and activity of the regulatory machinery for skeletal gene expression. Oncogene 2004;23(24):4315-29.
10. Meirelles Lda S, Fontes AM, Covas DT, Caplan AI. Mechanisms involved in the therapeutic properties of mesenchymal stem cells. Cytokine Growth Factor Rev 2009;20(5-6):419-27.
11. Long MW. Osteogenesis and bone-marrow-derived cells. Blood Cells Mol Dis 2001;27(3):677-90.
12. Uccelli A, Moretta L, Pistoia V. Mesenchymal stem cells in health and disease. Nat Rev Immunol 2008;8(9):726-36.
13. Xu J, Li Z, Hou Y, Fang W. Potential mechanisms underlying the Runx2 induced osteogenesis of bone marrow mesenchymal stem cells. Am J Transl Res 2015;7(12):2527-35.
14. Aubin JE. Bone stem cells. J Cell Biochem Suppl 1998;30-31:73-82.
15. Fratzl P, R W. Nature's hierarchial materials. Materials Science 2007;52(8):1263-1334.

16. Katagiri T, Takahashi N. Regulatory mechanisms of osteoblast and osteoclast differentiation. Oral Dis 2002;8(3):147-59.
17. Nakayachi M, Ito J, Hayashida C, Ohyama Y, Kakino A, Okayasu M, Sato T, Ogasawara T, Kaneda T, Suda N and others. Lectin-like oxidized low-density lipoprotein receptor-1 abrogation causes resistance to inflammatory bone destruction in mice, despite promoting osteoclastogenesis in the steady state. Bone 2015;75:170-82.
18. Theoleyre S, Wittrant Y, Tat SK, Fortun Y, Redini F, Heymann D. The molecular triad OPG/RANK/RANKL: involvement in the orchestration of pathophysiological bone remodeling. Cytokine Growth Factor Rev 2004;15(6):457-75.
19. Weiner S, H.D W. The material bone: Structure-Mechanical Function Relations. Materials Science 1998;28:271-298.
20. Ziv V, Wagner HD, Weiner S. Microstructure-microhardness relations in parallel-fibered and lamellar bone. Bone 1996;18(5):417-28.
21. Nudelman F, Pieterse K, George A, Bomans PH, Friedrich H, Brylka LJ, Hilbers PA, de With G, Sommerdijk NA. The role of collagen in bone apatite formation in the presence of hydroxyapatite nucleation inhibitors. Nat Mater 2010;9(12):1004-9.
22. Wang Y, Azais T, Robin M, Vallee A, Catania C, Legriel P, Pehau-Arnaudet G, Babonneau F, Giraud-Guille MM, Nassif N. The predominant role of collagen in the nucleation, growth, structure and orientation of bone apatite. Nat Mater 2012;11(8):724-33.
23. Boskey AL. Matrix proteins and mineralization: an overview. Connect Tissue Res 1996;35(1-4):357-63.
24. Schindeler A, McDonald MM, Bokko P, Little DG. Bone remodeling during fracture repair: The cellular picture. Semin Cell Dev Biol 2008;19(5):459-66.
25. Deschaseaux F, Sensebe L, Heymann D. Mechanisms of bone repair and regeneration. Trends Mol Med 2009;15(9):417-29.
26. Davis GE, Saunders WB. Molecular balance of capillary tube formation versus regression in wound repair: Role of matrix metalloproteinases and their inhibitors. Journal of Investigative Dermatology Symposium Proceedings 2006;11(1):44-56.
27. Loffek S, Schilling O, Franzke CW. Series "matrix metalloproteinases in lung health and disease": Biological role of matrix metalloproteinases: a critical balance. Eur Respir J 2011;38(1):191-208.
28. Kamimura D, Ishihara K, Hirano T. IL-6 signal transduction and its physiological roles: the signal orchestration model. Rev Physiol Biochem Pharmacol 2003;149:1-38.
29. Franchimont N, Wertz S, Malaise M. Interleukin-6: An osteotropic factor influencing bone formation? Bone 2005;37(5):601-6.

30. Cullinan MP, Westerman B, Hamlet SM, Palmer JE, Faddy MJ, Seymour GJ, Middleton PG, Taylor JJ. Progression of periodontal disease and interleukin-10 gene polymorphism. J Periodontal Res 2008;43(3):328-33.
31. Moore KW, de Waal Malefyt R, Coffman RL, O'Garra A. Interleukin-10 and the interleukin-10 receptor. Annu Rev Immunol 2001;19:683-765.
32. Iyer SS, Cheng G. Role of interleukin 10 transcriptional regulation in inflammation and autoimmune disease. Crit Rev Immunol 2012;32(1):23-63.
33. Kuziel WA, Morgan SJ, Dawson TC, Griffin S, Smithies O, Ley K, Maeda N. Severe reduction in leukocyte adhesion and monocyte extravasation in mice deficient in CC chemokine receptor 2. Proc Natl Acad Sci U S A 1997;94(22):12053-8.
34. Graves DT, Jiang Y, Valente AJ. The expression of monocyte chemoattractant protein-1 and other chemokines by osteoblasts. Front Biosci 1999;4:D571-80.
35. Baggiolini M, Loetscher P, Moser B. Interleukin-8 and the chemokine family. Int J Immunopharmacol 1995;17(2):103-8.
36. Driscoll KE. Macrophage inflammatory proteins: biology and role in pulmonary inflammation. Exp Lung Res 1994;20(6):473-90.
37. Fahey TJ, 3rd, Tracey KJ, Tekamp-Olson P, Cousens LS, Jones WG, Shires GT, Cerami A, Sherry B. Macrophage inflammatory protein 1 modulates macrophage function. J Immunol 1992;148(9):2764-9.
38. Liu M, Guo S, Hibbert JM, Jain V, Singh N, Wilson NO, Stiles JK. CXCL10/IP-10 in infectious diseases pathogenesis and potential therapeutic implications. Cytokine Growth Factor Rev 2011;22(3):121-30.
39. Nagase H, Miyamasu M, Yamaguchi M, Imanishi M, Tsuno NH, Matsushima K, Yamamoto K, Morita Y, Hirai K. Cytokine-mediated regulation of CXCR4 expression in human neutrophils. J Leukoc Biol 2002;71(4):711-7.
40. Zheng H, Fu G, Dai T, Huang H. Migration of endothelial progenitor cells mediated by stromal cell-derived factor-1alpha/CXCR4 via PI3K/Akt/eNOS signal transduction pathway. J Cardiovasc Pharmacol 2007;50(3):274-80.
41. Rahimi P, Wang CY, Stashenko P, Lee SK, Lorenzo JA, Graves DT. Monocyte chemoattractant protein-1 expression and monocyte recruitment in osseous inflammation in the mouse. Endocrinology 1995;136(6):2752-9.
42. Hocking AM. The Role of Chemokines in Mesenchymal Stem Cell Homing to Wounds. Adv Wound Care (New Rochelle) 2015;4(11):623-630.

43. Anderson JM, McNally AK. Biocompatibility of implants: lymphocyte/macrophage interactions. Semin Immunopathol 2011;33(3):221-33.
44. Hughes DE, Salter DM, Dedhar S, Simpson R. Integrin expression in human bone. J Bone Miner Res 1993;8(5):527-33.
45. Stewart M, Thiel M, Hogg N. Leukocyte integrins. Curr Opin Cell Biol 1995;7(5):690-6.
46. Van Lint P, Libert C. Chemokine and cytokine processing by matrix metalloproteinases and its effect on leukocyte migration and inflammation. J Leukoc Biol 2007;82(6):1375-81.
47. Gutierrez-Fernandez A, Inada M, Balbin M, Fueyo A, Pitiot AS, Astudillo A, Hirose K, Hirata M, Shapiro SD, Noel A and others. Increased inflammation delays wound healing in mice deficient in collagenase-2 (MMP-8). FASEB J 2007;21(10):2580-91.
48. Hasty KA, Jeffrey JJ, Hibbs MS, Welgus HG. The collagen substrate specificity of human neutrophil collagenase. J Biol Chem 1987;262(21):10048-52.
49. Pirila E, Korpi JT, Korkiamaki T, Jahkola T, Gutierrez-Fernandez A, Lopez-Otin C, Saarialho-Kere U, Salo T, Sorsa T. Collagenase-2 (MMP-8) and matrilysin-2 (MMP-26) expression in human wounds of different etiologies. Wound Repair Regen 2007;15(1):47-57.
50. Clarke B. Normal bone anatomy and physiology. Clin J Am Soc Nephrol 2008;3 Suppl 3:S131-9.
51. Lombardi G, Perego S, Luzi L, Banfi G. A four-season molecule: osteocalcin. Updates in its physiological roles. Endocrine 2015;48(2):394-404.
52. Jingushi S, Bolander ME. Biological Cascades of Fracture Healing as Models for Bone-Biomaterial Interface. In: Davies JE, editor. The Bone-Biomaterial Interface. Toronto: University of Toronto Press; 1990. p 250-262.
53. Letterio JJ, Roberts AB. Regulation of immune responses by TGF-beta. Annu Rev Immunol 1998;16:137-61.
54. Tang Y, Wu X, Lei W, Pang L, Wan C, Shi Z, Zhao L, Nagy TR, Peng X, Hu J and others. TGF-beta1-induced migration of bone mesenchymal stem cells couples bone resorption with formation. Nat Med 2009;15(7):757-65.
55. Sanchez-Capelo A. Dual role for TGF-beta1 in apoptosis. Cytokine Growth Factor Rev 2005;16(1):15-34.
56. Vaibhav B, Nilesh P, Vikram S, Anshul C. Bone morphogenic protein and its application in trauma cases: a current concept update. Injury 2007;38(11):1227-35.
57. Salazar VS, Gamer LW, Rosen V. BMP signalling in skeletal development, disease and repair. Nat Rev Endocrinol 2016;12(4):203-21.

58. Jung Y, Song J, Shiozawa Y, Wang J, Wang Z, Williams B, Havens A, Schneider A, Ge C, Franceschi RT and others. Hematopoietic stem cells regulate mesenchymal stromal cell induction into osteoblasts thereby participating in the formation of the stem cell niche. Stem Cells 2008;26(8):2042-51.
59. Cho TJ, Gerstenfeld LC, Einhorn TA. Differential temporal expression of members of the transforming growth factor beta superfamily during murine fracture healing. J Bone Miner Res 2002;17(3):513-20.
60. Komori T, Yagi H, Nomura S, Yamaguchi A, Sasaki K, Deguchi K, Shimizu Y, Bronson RT, Gao YH, Inada M and others. Targeted disruption of Cbfa1 results in a complete lack of bone formation owing to maturational arrest of osteoblasts. Cell 1997;89(5):755-64.
61. Charles JF, Aliprantis AO. Osteoclasts: more than 'bone eaters'. Trends in Molecular Medicine 2014;20(8):449-459.
62. Duong LT, Lakkakorpi P, Nakamura I, Rodan GA. Integrins and signaling in osteoclast function. Matrix Biol 2000;19(2):97-105.
63. Henriksen K, Karsdal MA, Martin TJ. Osteoclast-derived coupling factors in bone remodeling. Calcif Tissue Int 2014;94(1):88-97.
64. Pederson L, Ruan M, Westendorf JJ, Khosla S, Oursler MJ. Regulation of bone formation by osteoclasts involves Wnt/BMP signaling and the chemokine sphingosine-1-phosphate. Proc Natl Acad Sci U S A 2008;105(52):20764-9.
65. Littlewood-Evans A, Kokubo T, Ishibashi O, Inaoka T, Wlodarski B, Gallagher JA, Bilbe G. Localization of cathepsin K in human osteoclasts by in situ hybridization and immunohistochemistry. Bone 1997;20(2):81-6.
66. Perez-Amodio S, Beertsen W, Everts V. (Pre-)osteoclasts induce retraction of osteoblasts before their fusion to osteoclasts. J Bone Miner Res 2004;19(10):1722-31.
67. Anderson DM, Maraskovsky E, Billingsley WL, Dougall WC, Tometsko ME, Roux ER, Teepe MC, DuBose RF, Cosman D, Galibert L. A homologue of the TNF receptor and its ligand enhance T-cell growth and dendritic-cell function. Nature 1997;390(6656):175-9.
68. Wong BR, Rho JR, Arron J, Robinson E, Orlinick J, Chao M, Kalachikov S, Cayani E, Bartlett FS, Frankel WN and others. TRANCE is a novel ligand of the tumor necrosis factor receptor family that activates c-Jun N-terminal kinase in T cells. Journal of Biological Chemistry 1997;272(40):25190-25194.
69. Larsson C, Esposito M, Liao H, Thomsen P. The Titanium-Bone Interface In Vivo. In: Brunette DM, Tengvall P, Textor M, Thomsen P, editors. Titanium in Medicine. New York: Springer; 2001. p 587-648.

70. Thomsen P, Ericson LE. Inflammatory Cell Response to Bone Implant Surfaces. In: Davies JE, editor. The Bone-Biomaterial Interface. Toronto: University of Toronto Press; 1991. p 153-169.
71. Hong J, Azens A, Ekdahl KN, Granqvist CG, Nilsson B. Material-specific thrombin generation following contact between metal surfaces and whole blood. Biomaterials 2005;26(12):1397-403.
72. Nilsson PH, Ekdahl KN, Magnusson PU, Qu H, Iwata H, Ricklin D, Hong J, Lambris JD, Nilsson B, Teramura Y. Autoregulation of thromboinflammation on biomaterial surfaces by a multicomponent therapeutic coating. Biomaterials 2013;34(4):985-94.
73. Zipfel PF, Skerka C. Complement regulators and inhibitory proteins. Nat Rev Immunol 2009;9(10):729-40.
74. Sennerby L, Thomsen P, Ericson LE. Early tissue response to titanium implants inserted in rabbit cortical bone. Part I *Light microscopic observations*. Journal of Materials Science: Materials in Medicine 1993;4(3):240-250.
75. Sennerby L, Thomsen P, Ericson LE. Early tissue response to titanium implants inserted in rabbit cortical bone. Part II *Ultrastructural observations*. Journal of Materials Science: Materials in Medicine 1993;4(5):494-502.
76. Nakashima Y, Sun DH, Trindade MC, Chun LE, Song Y, Goodman SB, Schurman DJ, Maloney WJ, Smith RL. Induction of macrophage C-C chemokine expression by titanium alloy and bone cement particles. J Bone Joint Surg Br 1999;81(1):155-62.
77. Refai AK, Textor M, Brunette DM, Waterfield JD. Effect of titanium surface topography on macrophage activation and secretion of proinflammatory cytokines and chemokines. J Biomed Mater Res A 2004;70(2):194-205.
78. Lu WL, Wang N, Gao P, Li CY, Zhao HS, Zhang ZT. Effects of anodic titanium dioxide nanotubes of different diameters on macrophage secretion and expression of cytokines and chemokines. Cell Prolif 2015;48(1):95-104.
79. Sinha RK, Tuan RS. Regulation of human osteoblast integrin expression by orthopedic implant materials. Bone 1996;18(5):451-7.
80. ter Brugge PJ, Torensma R, De Ruijter JE, Figdor CG, Jansen JA. Modulation of integrin expression on rat bone marrow cells by substrates with different surface characteristics. Tissue Eng 2002;8(4):615-26.
81. Woodruff MA, Jones P, Farrar D, Grant DM, Scotchford CA. Human osteoblast cell spreading and vinculin expression upon biomaterial surfaces. J Mol Histol 2007;38(5):491-9.
82. Luthen F, Lange R, Becker P, Rychly J, Beck U, Nebe JG. The influence of surface roughness of titanium on beta1- and beta3-integrin adhesion and the organization of fibronectin in human osteoblastic cells. Biomaterials 2005;26(15):2423-40.

83. Keselowsky BG, Wang L, Schwartz Z, Garcia AJ, Boyan BD. Integrin alpha(5) controls osteoblastic proliferation and differentiation responses to titanium substrates presenting different roughness characteristics in a roughness independent manner. J Biomed Mater Res A 2007;80(3):700-10.
84. Wang L, Zhao G, Olivares-Navarrete R, Bell BF, Wieland M, Cochran DL, Schwartz Z, Boyan BD. Integrin beta1 silencing in osteoblasts alters substrate-dependent responses to 1,25-dihydroxy vitamin D3. Biomaterials 2006;27(20):3716-25.
85. Takebe J, Champagne CM, Offenbacher S, Ishibashi K, Cooper LF. Titanium surface topography alters cell shape and modulates bone morphogenetic protein 2 expression in the J774A.1 macrophage cell line. J Biomed Mater Res A 2003;64(2):207-16.
86. Guo J, Padilla RJ, Ambrose W, De Kok IJ, Cooper LF. The effect of hydrofluoric acid treatment of TiO2 grit blasted titanium implants on adherent osteoblast gene expression in vitro and in vivo. Biomaterials 2007;28(36):5418-25.
87. Monjo M, Lamolle SF, Lyngstadaas SP, Ronold HJ, Ellingsen JE. In vivo expression of osteogenic markers and bone mineral density at the surface of fluoride-modified titanium implants. Biomaterials 2008;29(28):3771-80.
88. Boyan BD, Dean DD, Lohmann CH, Cochran DL, Sylvia VL, Schwartz Z. The Titanium-Bone Cell Interface In Vitro: The Role of the Surface in Promoting Osteointegration. In: Brunette DM, Tengvall P, Textor M, Thomsen P, editors. Titanium in Medicine. New York: Springer; 2001. p 561-585.
89. Dhert WJ, Thomsen P, Blomgren AK, Esposito M, Ericson LE, Verbout AJ. Integration of press-fit implants in cortical bone: a study on interface kinetics. J Biomed Mater Res 1998;41(4):574-83.
90. Taxt-Lamolle SF, Rubert M, Haugen HJ, Lyngstadaas SP, Ellingsen JE, Monjo M. Controlled electro-implementation of fluoride in titanium implant surfaces enhances cortical bone formation and mineralization. Acta Biomater 2010;6(3):1025-32.
91. Monjo M, Ramis JM, Ronold HJ, Taxt-Lamolle SF, Ellingsen JE, Lyngstadaas SP. Correlation between molecular signals and bone bonding to titanium implants. Clin Oral Implants Res 2013;24(9):1035-43.
92. Branemark R, Berlin O, Hagberg K, Bergh P, Gunterberg B, Rydevik B. A novel osseointegrated percutaneous prosthetic system for the treatment of patients with transfemoral amputation: A prospective study of 51 patients. Bone Joint J 2014;96-b(1):106-13.
93. Jeyapalina S, Beck JP, Bachus KN, Bloebaum RD. Cortical bone response to the presence of load-bearing percutaneous osseointegrated prostheses. Anat Rec (Hoboken) 2012;295(9):1437-45.

94. Juhnke DL, Beck JP, Jeyapalina S, Aschoff HH. Fifteen years of experience with Integral-Leg-Prosthesis: Cohort study of artificial limb attachment system. J Rehabil Res Dev 2015;52(4):407-20.
95. Khemka A, FarajAllah CI, Lord SJ, Bosley B, Al Muderis M. Osseointegrated total hip replacement connected to a lower limb prosthesis: a proof-of-concept study with three cases. J Orthop Surg Res 2016;11(1):13.
96. Schalk SA, Jonkergouw N, van der Meer F, Swaan WM, Aschoff HH, van der Wurff P. The Evaluation of Daily Life Activities after Application of an Osseointegrated Prosthesis Fixation in a Bilateral Transfemoral Amputee: A Case Study. Medicine (Baltimore) 2015;94(36):e1416.
97. Tillander J, Hagberg K, Hagberg L, Branemark R. Osseointegrated titanium implants for limb prostheses attachments: infectious complications. Clin Orthop Relat Res 2010;468(10):2781-8.
98. Moojen DJ, Spijkers SN, Schot CS, Nijhof MW, Vogely HC, Fleer A, Verbout AJ, Castelein RM, Dhert WJ, Schouls LM. Identification of orthopaedic infections using broad-range polymerase chain reaction and reverse line blot hybridization. J Bone Joint Surg Am 2007;89(6):1298-305.
99. Moojen DJ, van Hellemondt G, Vogely HC, Burger BJ, Walenkamp GH, Tulp NJ, Schreurs BW, de Meulemeester FR, Schot CS, van de Pol I and others. Incidence of low-grade infection in aseptic loosening of total hip arthroplasty. Acta Orthop 2010;81(6):667-73.
100. Donath K, Breuner G. A method for the study of undecalcified bones and teeth with attached soft tissues. The Sage-Schliff (sawing and grinding) technique. J Oral Pathol 1982;11(4):318-26.
101. Jarmar T, Palmquist A, Branemark R, Hermansson L, Engqvist H, Thomsen P. Characterization of the surface properties of commercially available dental implants using scanning electron microscopy, focused ion beam, and high-resolution transmission electron microscopy. Clin Implant Dent Relat Res 2008;10(1):11-22.
102. Palmquist A, Lindberg F, Emanuelsson L, Branemark R, Engqvist H, Thomsen P. Biomechanical, histological, and ultrastructural analyses of laser micro- and nano-structured titanium alloy implants: a study in rabbit. J Biomed Mater Res A 2010;92(4):1476-86.
103. Branemark R, Ohrnell LO, Nilsson P, Thomsen P. Biomechanical characterization of osseointegration during healing: an experimental in vivo study in the rat. Biomaterials 1997;18(14):969-78.
104. Branemark R, Skalak R. An in-vivo method for biomechanical characterization of bone-anchored implants. Med Eng Phys 1998;20(3):216-9.
105. Rosengren A, Johansson BR, Thomsen P, Ericson LE. Method for immunolocalization of extracellular proteins in association with the implant-soft tissue interface. Biomaterials 1994;15(1):17-24.

106. Hunt JA, McLaughlin PJ, Flanagan BF. Techniques to investigate cellular and molecular interactions in the host response to implanted biomaterials. Biomaterials 1997;18:1449-1459.
107. Neo M, Voigt CF, Herbst H, Gross UM. Analysis of osteoblast activity at biomaterial-bone interfaces by in situ hybridization. Journal of Biomedical Materials Research 1996;30(4):485-492.
108. Song G, Habibovic P, Bao C, Hu J, van Blitterswijk CA, Yuan H, Chen W, Xu HH. The homing of bone marrow MSCs to non-osseous sites for ectopic bone formation induced by osteoinductive calcium phosphate. Biomaterials 2013;34(9):2167-76.
109. Dogan SB, Kurtis MB, Tuter G, Serdar M, Watanabe K, Karakis S. Evaluation of Clinical Parameters and Levels of Proinflammatory Cytokines in the Crevicular Fluid Around Dental Implants in Patients with Type 2 Diabetes Mellitus. Int J Oral Maxillofac Implants 2015;30(5):1119-27.
110. Yaghobee S, Khorsand A, Rasouli Ghohroudi AA, Sanjari K, Kadkhodazadeh M. Assessment of interleukin-1beta and interleukin-6 in the crevicular fluid around healthy implants, implants with peri-implantitis, and healthy teeth: a cross-sectional study. J Korean Assoc Oral Maxillofac Surg 2014;40(5):220-4.
111. Turri A, Elgali I, Vazirisani F, Johansson A, Emanuelsson L, Dahlin C, Thomsen P, Omar O. Guided bone regeneration is promoted by the molecular events in the membrane compartment. Biomaterials 2016;84:167-83.
112. Yang P, Huang X, Wang C, Dang X, Wang K. Repair of bone defects using a new biomimetic construction fabricated by adipose-derived stem cells, collagen I, and porous beta-tricalcium phosphate scaffolds. Exp Biol Med (Maywood) 2013;238(12):1331-43.
113. Pfaffl MW. Relative quantifications. In: Dorak TM, editor. Real-time PCR. Cornwall: Taylor & Francis Group; 2006. p 63-80.
114. Bustin SA, Benes V, Garson JA, Hellemans J, Huggett J, Kubista M, Mueller R, Nolan T, Pfaffl MW, Shipley GL and others. The MIQE guidelines: minimum information for publication of quantitative real-time PCR experiments. Clin Chem 2009;55(4):611-22.
115. Gallup JM, Sow FB, Van Geelen A, Ackermann MR. SPUD qPCR assay confirms PREXCEL-Q softwares ability to avoid qPCR inhibition. Curr Issues Mol Biol 2010;12(3):129-34.
116. Stahlberg A, Hakansson J, Xian X, Semb H, Kubista M. Properties of the reverse transcription reaction in mRNA quantification. Clin Chem 2004;50(3):509-15.
117. Huggett J, Dheda K, Bustin SA. Normalization. In: Dorak TM, editor. Real-time PCR. Cornwall: Taylor & Francis Group; 2006. p 83-90.
118. Pfaffl MW. A new mathematical model for relative quantification in real-time RT-PCR. Nucleic Acids Res 2001;29(9):e45.

119. Wang X, Seed B. High-throughput primer and probe design. In: Dorak TM, editor. Real-time PCR. Cornwall: Taylor & Francis Group; 2006. p 93-105.
120. Assarsson E, Lundberg M, Holmquist G, Bjorkesten J, Thorsen SB, Ekman D, Eriksson A, Rennel Dickens E, Ohlsson S, Edfeldt G and others. Homogenous 96-plex PEA immunoassay exhibiting high sensitivity, specificity, and excellent scalability. PLoS One 2014;9(4):e95192.
121. Lundberg M, Eriksson A, Tran B, Assarsson E, Fredriksson S. Homogeneous antibody-based proximity extension assays provide sensitive and specific detection of low-abundant proteins in human blood. Nucleic Acids Res 2011;39(15):e102.
122. Hunt JA, Rhodes NP, Williams DF. Analysis of the inflammatory exudate surrounding implanted polymers using flow cytometry. Journal of Materials Science: Materials in Medicine 1995;6(12):839-843.
123. Ovrenovits M, Pakos EE, Vartholomatos G, Paschos NK, Xenakis TA, Mitsionis GI. Flow cytometry as a diagnostic tool for identifying total hip arthroplasty loosening and differentiating between septic and aseptic cases. Eur J Orthop Surg Traumatol 2015;25(7):1153-9.
124. Rozen S, Skaletsky H. Primer3 on the WWW for general users and for biologist programmers. Methods Mol Biol 2000;132:365-86.
125. Granero-Molto F, Weis JA, Miga MI, Landis B, Myers TJ, O'Rear L, Longobardi L, Jansen ED, Mortlock DP, Spagnoli A. Regenerative effects of transplanted mesenchymal stem cells in fracture healing. Stem Cells 2009;27(8):1887-98.
126. Otsuru S, Tamai K, Yamazaki T, Yoshikawa H, Kaneda Y. Circulating bone marrow-derived osteoblast progenitor cells are recruited to the bone-forming site by the CXCR4/stromal cell-derived factor-1 pathway. Stem Cells 2008;26(1):223-34.
127. Ekdahl KN, Lambris JD, Elwing H, Ricklin D, Nilsson PH, Teramura Y, Nicholls IA, Nilsson B. Innate immunity activation on biomaterial surfaces: a mechanistic model and coping strategies. Adv Drug Deliv Rev 2011;63(12):1042-50.
128. Gorbet MB, Sefton MV. Biomaterial-associated thrombosis: roles of coagulation factors, complement, platelets and leukocytes. Biomaterials 2004;25(26):5681-703.
129. Shiu HT, Goss B, Lutton C, Crawford R, Xiao Y. Formation of blood clot on biomaterial implants influences bone healing. Tissue Eng Part B Rev 2014;20(6):697-712.
130. Eskin SG, Horbett TA, McIntire LV, Mitchell RN, Ratner BD, Schoen FJ, Yee A. Biology, Biochemistry and Medicine. Biomaterials science: An introduction to materials in medicine. China: Elsevier; 2004. p 237-282.

131. Tang L, Eaton JW. Fibrin(ogen) mediates acute inflammatory responses to biomaterials. J Exp Med 1993;178(6):2147-56.
132. Brunette DM. Principles of Cell Behavior on Titanium Surfaces and their Application to Implanted Devices. In: Brunette DM, Tengvall P, Textor M, Thomsen P, editors. Titanium in Medicine. New York: Springer; 2001. p 485-512.
133. Chou L, Firth JD, Uitto VJ, Brunette DM. Effects of titanium substratum and grooved surface topography on metalloproteinase-2 expression in human fibroblasts. J Biomed Mater Res 1998;39(3):437-45.
134. Soskolne WA, Cohen S, Sennerby L, Wennerberg A, Shapira L. The effect of titanium surface roughness on the adhesion of monocytes and their secretion of TNF-alpha and PGE2. Clin Oral Implants Res 2002;13(1):86-93.
135. Zink C, Hall H, Brunette DM, Spencer ND. Orthogonal nanometer-micrometer roughness gradients probe morphological influences on cell behavior. Biomaterials 2012;33(32):8055-61.
136. Ogawa T, Nishimura I. Different bone integration profiles of turned and acid-etched implants associated with modulated expression of extracellular matrix genes. Int J Oral Maxillofac Implants 2003;18(2):200-10.
137. Setzer B, Bachle M, Metzger MC, Kohal RJ. The gene-expression and phenotypic response of hFOB 1.19 osteoblasts to surface-modified titanium and zirconia. Biomaterials 2009;30(6):979-90.
138. Hayashi H, Nakahama K, Sato T, Tuchiya T, Asakawa Y, Maemura T, Tanaka M, Morita M, Morita I. The role of Mac-1 (CD11b/CD18) in osteoclast differentiation induced by receptor activator of nuclear factor-kappaB ligand. FEBS Lett 2008;582(21-22):3243-8.
139. Omar O. Mechanisms of Osseointegration: Experimental Studies on Early Cellular and Molecular Events in vivo [Doctoral Thesis]. Gothenburg: University of Gothenburg; 2010.
140. Waterman RS, Tomchuck SL, Henkle SL, Betancourt AM. A new mesenchymal stem cell (MSC) paradigm: polarization into a pro-inflammatory MSC1 or an Immunosuppressive MSC2 phenotype. PLoS One 2010;5(4):e10088.
141. Jeannin P, Duluc D, Delneste Y. IL-6 and leukemia-inhibitory factor are involved in the generation of tumor-associated macrophage: regulation by IFN-gamma. Immunotherapy 2011;3(4 Suppl):23-6.
142. Nicola NA, Babon JJ. Leukemia inhibitory factor (LIF). Cytokine Growth Factor Rev 2015;26(5):533-44.
143. Walker EC, McGregor NE, Poulton IJ, Solano M, Pompolo S, Fernandes TJ, Constable MJ, Nicholson GC, Zhang JG, Nicola NA and others. Oncostatin M promotes bone formation independently of resorption when signaling through leukemia inhibitory factor

receptor in mice. Journal of Clinical Investigation 2010;120(2):582-592.
144. Crescioli C. Chemokines and transplant outcome. Clin Biochem 2016;49(4-5):355-62.
145. Anderson JM, Rodriguez A, Chang DT. Foreign body reaction to biomaterials. Semin Immunol 2008;20(2):86-100.
146. Thomsen P, Gretzer C. Macrophage interactions with modified material surfaces. Curr Opin Solid State Mater Sci 2001;5(2–3):163-176.
147. Tsaryk R, Peters K, Barth S, Unger RE, Scharnweber D, Kirkpatrick CJ. The role of oxidative stress in pro-inflammatory activation of human endothelial cells on Ti6Al4V alloy. Biomaterials 2013;34(33):8075-85.
148. Suska F, Esposito M, Gretzer C, Kalltorp M, Tengvall P, Thomsen P. IL-1alpha, IL-1beta and TNF-alpha secretion during in vivo/ex vivo cellular interactions with titanium and copper. Biomaterials 2003;24(3):461-8.
149. Elgali I, Igawa K, Palmquist A, Lenneras M, Xia W, Choi S, Chung UI, Omar O, Thomsen P. Molecular and structural patterns of bone regeneration in surgically created defects containing bone substitutes. Biomaterials 2014;35(10):3229-42.
150. Walsh MC, Choi Y. Biology of the RANKL-RANK-OPG System in Immunity, Bone, and Beyond. Front Immunol 2014;5:511.
151. Albrektsson T, Wennerberg A. Oral implant surfaces: Part 1--review focusing on topographic and chemical properties of different surfaces and in vivo responses to them. Int J Prosthodont 2004;17(5):536-43.
152. Cooper LF, Zhou YS, Takebe J, Guo JL, Abron A, Holmen A, Ellingsen JE. Fluoride modification effects on osteoblast behavior and bone formation at TiO2 grit-blasted c.p. titanium endosseous implants. Biomaterials 2006;27(6):926-936.
153. Meng W, Zhou Y, Zhang Y, Cai Q, Yang L, Wang B. Effects of hierarchical micro/nano-textured titanium surface features on osteoblast-specific gene expression. Implant Dent 2013;22(6):656-61.
154. Ramis JM, Taxt-Lamolle SF, Lyngstadaas SP, Reseland JE, Ellingsen JE, Monjo M. Identification of early response genes to roughness and fluoride modification of titanium implants in human osteoblasts. Implant Dent 2012;21(2):141-9.
155. Karazisis D, Ballo AM, Petronis S, Agheli H, Emanuelsson L, Thomsen P, Omar O. The role of well-defined nanotopography of titanium implants on osseointegration: cellular and molecular events in vivo. Int J Nanomedicine 2016;11:1367-82.
156. Zhao G, Schwartz Z, Wieland M, Rupp F, Geis-Gerstorfer J, Cochran DL, Boyan BD. High surface energy enhances cell response to

titanium substrate microstructure. J Biomed Mater Res A 2005;74(1):49-58.
157. Larsson C, Thomsen P, Aronsson BO, Rodahl M, Lausmaa J, Kasemo B, Ericson LE. Bone response to surface-modified titanium implants: studies on the early tissue response to machined and electropolished implants with different oxide thicknesses. Biomaterials 1996;17(6):605-16.
158. Sul YT, Johansson C, Wennerberg A, Cho LR, Chang BS, Albrektsson T. Optimum surface properties of oxidized implants for reinforcement of osseointegration: surface chemistry, oxide thickness, porosity, roughness, and crystal structure. Int J Oral Maxillofac Implants 2005;20(3):349-59.
159. Hagberg K, Hansson E, Branemark R. Outcome of percutaneous osseointegrated prostheses for patients with unilateral transfemoral amputation at two-year follow-up. Arch Phys Med Rehabil 2014;95(11):2120-7.
160. Holgers KM, Tjellstrom A, Bjursten LM, Erlandsson BE. Soft tissue reactions around percutaneous implants: a clinical study of soft tissue conditions around skin-penetrating titanium implants for bone-anchored hearing aids. Am J Otol 1988;9(1):56-9.
161. Nebergall A, Bragdon C, Antonellis A, Karrholm J, Branemark R, Malchau H. Stable fixation of an osseointegated implant system for above-the-knee amputees: titel RSA and radiographic evaluation of migration and bone remodeling in 55 cases. Acta Orthop 2012;83(2):121-8.
162. Ettinger M, Calliess T, Kielstein JT, Sibai J, Bruckner T, Lichtinghagen R, Windhagen H, Lukasz A. Circulating biomarkers for discrimination between aseptic joint failure, low-grade infection, and high-grade septic failure. Clin Infect Dis 2015;61(3):332-41.
163. Grant MM, Monksfield P, Proops D, Brine M, Addison O, Sammons RL, Matthews JB, Reid A, Chapple IL. Fluid exudates from inflamed bone-anchored hearing aids demonstrate elevated levels of cytokines and biomarkers of tissue and bone metabolism. Otol Neurotol 2010;31(3):433-9.
164. Duarte PM, de Mendonca AC, Maximo MB, Santos VR, Bastos MF, Nociti FH. Effect of anti-infective mechanical therapy on clinical parameters and cytokine levels in human peri-implant diseases. J Periodontol 2009;80(2):234-43.
165. Liskmann S, Vihalemm T, Salum O, Zilmer K, Fischer K, Zilmer M. Correlations between clinical parameters and interleukin-6 and interleukin-10 levels in saliva from totally edentulous patients with peri-implant disease. International Journal of Oral & Maxillofacial Implants 2006;21(4):543-550.
166. Pigossi SC, Alvim-Pereira F, Montes CC, Finoti LS, Secolin R, Trevilatto PC, Scarel-Caminaga RM. Genetic association study

between Interleukin 10 gene and dental implant loss. Arch Oral Biol 2012;57(9):1256-63.
167. Couper KN, Blount DG, Riley EM. IL-10: the master regulator of immunity to infection. J Immunol 2008;180(9):5771-7.
168. Garlet GP, Martins W, Jr., Fonseca BA, Ferreira BR, Silva JS. Matrix metalloproteinases, their physiological inhibitors and osteoclast factors are differentially regulated by the cytokine profile in human periodontal disease. J Clin Periodontol 2004;31(8):671-9.
169. DeDent AC, McAdow M, Schneewind O. Distribution of protein A on the surface of Staphylococcus aureus. J Bacteriol 2007;189(12):4473-84.
170. Stavropoulos A, Sculean A, Bosshardt DD, Buser D, Klinge B. Pre-clinical in vivo models for the screening of bone biomaterials for oral/craniofacial indications: focus on small-animal models. Periodontol 2000 2015;68(1):55-65.
171. Omar OM, Graneli C, Ekstrom K, Karlsson C, Johansson A, Lausmaa J, Wexell CL, Thomsen P. The stimulation of an osteogenic response by classical monocyte activation. Biomaterials 2011;32(32):8190-204.
172. German MJ, Osei-Bempong C, Knuth CA, Deehan DJ, Oldershaw RA. Investigating the biological response of human mesenchymal stem cells to titanium surfaces. J Orthop Surg Res 2014;9:135.